Effects of hyperglycaemia on nucleocytoplasmic O-linked glycosylation in HUVEC

Astri Jeanette Meen

Master Thesis in Clinical Nutrition

Department of Nutrition

Institute of Basic Medical Sciences

UNIVERSITETET I OSLO

August 2008

Acknowledgements

The present work was conducted at the Department of Nutrition, University of Oslo in the laboratory of Professor Svein Olav Kolset.

I would like to thank my supervisor Senior Scientist Line Mariann Grønning-Wang for sharing your knowledge of O-GlcNAcylation, for fruitful discussions and enthusiasm and for always being available.

I would like to thank Svein Olav Kolset and all the members of the glycobiology group for creating such a nice and pleasant atmosphere.

A special thank to Parvin and Van for technical support in the lab and for always being helpful.

Many thanks also to Trine, my fellow student in the glycobiology group for valuable advice and encouragement. Finally many thanks to all my friends in H-03.

Oslo, July 2008

Astri Jeanette Meen

Summary

Diabetic patients have 2-4 fold increased risk of cardiovascular disease events, and have about 60 % increased risk of early mortality. Endothelial cells are sensitive for a hyperglycaemic environment. Excess glucose entering the hexosamine pathway is thought to elevate O-linked glycosylation (O-GlcNAcylation) of various nucleocytoplasmic proteins leading to endothelial dysfunction, insulin resistance, diabetes and diabetic complications.

Numerous transcription factors are regulated by O-GlcNAcylation. Glucose was recently reported to function as a direct agonist of the transcription factor liver X receptor (LXR). However, direct binding of the hydrophilic glucose molecule to the hydrophobic pocket in LXR suggests that glucose may rather act via downstream glucose signalling pathways. Preliminary data in our group indicates that LXRβ is target for O-GlcNAcylation in response to glucose in human THP-1 macrophages and HepG2 cells. O-GlcNAcylation prediction search (1) reveal several potential LXR O-GlcNAc sites.

The expression of the Id (inhibitors of DNA binding and differentiation) transcription repressors are increased in atherosclerosis and inflammation. D-glucose is shown to regulate Id1 protein expression in some cell types and previous work in our group have shown that Id2 is up-regulated by hyperglycaemia via the hexosamine signalling pathway and is a target for O-GlcNAcylation in J774.2 murine macrophages. The effects of D-glucose and O-GlcNAcylation of LXR and Id proteins in human endothelial cells have not previously been studied.

The aims of this master thesis were to study the effects of D-glucose and the O-GlcNAcase inhibitor NAG-thiazoline on overall protein O-GlcNAcylation level in HUVEC. Specific aims were to study whether LXR and Id are targets for O-GlcNAc modification and whether Id protein levels are regulated by hyperglycaemia. All experiments were performed in human umbilical vein endothelial cells (HUVEC).

Endothelial cells from human umbilical cords were isolated and cultured in vitro. The cells were incubated with D-glucose (1, 2.5, 5 or 25 mM) or NAG-thiazoline (10, 20 or 40 μM) for different times and whole cell lysates or nuclear extracts were prepared. N- and O-GlcNAcylated proteins were precipitated using succinylated wheat germ agglutinin (sWGA). Id or LXRβ proteins were immunoprecipitated by their respective antibodies. Finally, samples were separated by SDS-PAGE and total O-GlcNAcylated protein level, Id1, Id2, Id3, LXRα/β and LXRβ protein expression were determined by western blotting.

We revealed that NAG-thiazoline is 10 times more potent than PUGNAc, and 10 μM is enough to induce overall protein O-GlcNAcylation levels in HUVEC. Furthermore, our data indicates that Id1 is a target for O-GlcNAcylation, and Id1 protein expression is in contrast to Id3 not up-regulated by D-glucose and NAG-thiazoline. LXRβ is a promising target for O-GlcNAcylation. However, further experiments are needed in order to make firm conclusions.

Table of contenst

List of abbreviations

ABCA-1	ATP binding cassette transporter 1
AEBSF	4-(2-Aminoethyl) benzenesulfonyl fluoride hydrochloride
AGE	Advanced glycosylation end-product
ALLN	N-acetyl-L-leucinal-L-leucinal-L-norleucinal
AMPK	AMP-activated protein kinase
BAEC	Bovine aortic endothelial cells
BCA	Bicinchoninic acid
bHLH	Basic helix-loop-helix
BSA	Bovine serum albumin
cAMP	Cyclic adenosine 3,´5´-monophosphate
CTD	C-terminal domain
DAG	Diacylglycerol
DON	6-diazo-5-oxo-norleucine
DTT	Dithiothreitol
EBM	Endothelial basal medium
ECL	Enhanced chemiluminescence
ECM	Extracellular matrix
EDTA	Ethylenediaminetetraacetic acid
EGF	Epidermal growth factor
eNOS	Endothelial nitric oxide synthase
FBS	Foetal bovine serum
FGF	Fibroblast growth factor
GAPDH	Glyceraldehyde-3 phosphate dehydrogenase
GFAT	L-glutamine:D-fructose-6-phosphate amidotransferase
GlcNAc	N-acetylglucosamine

Glucosamine-6-P	Glucosamine-6-phosphate
GLUT	Glucose transporter
HAEC	Human aortic endothelial cells
HCEC	Human coronary endothelial cells
HLH	Helix-Loop-Helix
HRP	Horse radish peroxide
HSL	Hormone sensitive lipase
HUVEC	Human Umbilical Vein Endothelial Cells
Id	Inhibitor of differentiation and DNA-binding
IgG	Immunoglobulin G
IgM	Immunoglobulin M
IRS	Insulin receptor substrate
kDa	Kilo dalton
LDL	Low-density lipoprotein
LXR	Liver X receptor
$MgCl_2$	Magnesium chloride
MMP	Matrix metalloproteinases
mOGT	Mitochondrial β-N-acetylglycosaminyl transferase
mRNA	Messenger ribonucleic acid
NAD+	Nicotinamide adenine dinucleotide
NADPH	Nicotinamide adenine dinucleotide phosphate
NaF	Sodium fluoride
NAG-thiazoline	1,2-dideoxy-2′methyl-α-D-glucopyranoso[2,1-*d*]-Δ2′-thiazoline
Na_3VO_4	Sodium orthovanadate
NaPPi	Sodium pyrophosphate
ncOGT	Nucleocytoplasmic β-N-acetylglycosaminyl transferase
NF-κB	Nuclear factor-κB

NO	Nitric oxide
OGT	O-linked-N-acetylglucosaminyl (GlcNAc) transferase
oxLDL	Oxidized low density lipoproteins
p53	Protein 53
PBS	Phosphate buffered saline
PI3K	Phosphatidylinositol-3-kinase
PKA	Protein kinase A
PKC	Protein kinase C
PUGNAc	O-(2-acetamido-2-deoxy-D-glucopyranosylidene)amino-N-phenylcarbamate
PVDF	Polyvinylidene fluoride
RAGE	AGE receptor
RCF	Relative centrifugal force
RIPA	Radio-Immunoprecipitation Assay
ROS	Reactive oxygen species
RPM	Rotations per minute
RXR	Retinoid X receptor
SDS	Sodium dodecyl sulfate
SDS-PAGE	Sodium dodecyl sulfate polyacrylamide gel electrophoresis
SP1	Selective promoter transcription factor-1
SREBP-1	Sterol regulatory element binding protein-1
STZ	Streptozotocin
TNF	Tumor necrosis factor
TPR	Tetratricopeptide repeat
UDP	Uridine diphosphate
VCAM-1	Vascular cell adhesion molecule-1
VSMC	Vascular smooth muscle cells
WHO	World Health Organization

1. Introduction

The cells use energy continuously, but the body experiences alternate food supply and fasting. The brain, red blood cells and renal medulla require glucose as their energy source and need a stable supply of glucose for normal function (2;3). The blood glucose is stabilized close to 5 mM determined mainly by the ratio between insulin and the counteracting hormones glucagon, cortisol, epinephrine and growth hormone (3).

Glucose absorbed from meals is the main stimulus for insulin secretion. Insulin is an anabolic hormone produced by the pancreatic β-cells. Insulin stimulates uptake of glucose into adipose tissue and muscle, favours the synthesis of glycogen (in liver and muscle), triacylglycerols (in adipose tissue and liver) and proteins (in most tissues) (3). Insulin also interacts with receptors in hypothalamus repressing anabolic signals while simultaneously activating catabolic signals (4).

Hyperglycaemia is first manifested as an elevation of postprandial blood glucose caused by insulin resistance in target tissues, leading to reduced glucose uptake in muscle, adipose tissue and liver and increased glucose production by the liver and kidney. Insulin resistance in adipocytes leads to increased level of free fatty acids in the circulation, and increased transport of free fatty acids into muscle, liver and β-cells further impairs insulin secretion and insulin action (5;6). Insulin resistance in hypothalamus causes hyperphagia and weight gain (4) thus establishing a vicious circle.

Insulin resistance generally leads to compensatory insulin production leading to hyperinsulinemia (7). When the pancreas is unable to produce enough insulin to meet the increased need, the blood glucose will rise (8) and eventually diabetes develops.

Hyperglycaemia is a characteristic feature of diabetes mellitus, and the current diagnostic criteria for diabetes mellitus as stated by WHO are fasting plasma glucose $\geq$ 7.0 mM or $\geq$ 11.1 mM in venous plasma two hours after ingestion of 75 gram

glucose (9). The group diagnosed by these criteria has a significantly increased risk of micro- and macrovascular complications and premature mortality (10).

The consumption of refined sugars has increased considerable during the last decades (11). In general, refined sugars (sucrose, fructose, glucose, starch hydrolysates, i.e. glucose syrup, high-fructose syrup etc.), are absorbed more rapidly than carbohydrates from starch or fibre containing foods, resulting in a rapid increase in the blood glucose (12;13). The postprandial glucose concentration in healthy individuals may reach 7-8 mM (14-16). Even healthy people experiencing repeated postprandial hyperglycaemic peaks have increased risk of cardiovascular diseases (15;17;18).

1.1 Endothelial cells and hyperglycaemia

Most cell types are able to reduce their uptake of glucose during periods of hyperglycaemia, and their intracellular glucose concentrations remains nearly constant. Endothelial cells are however, not able to control their uptake of glucose, and thus extracellular hyperglycaemia leads to intracellular hyperglycaemia (19;20).

Endothelial cells form a barrier (the endothelium) between the vascular smooth muscle cells (VSMC) and the blood constituents. Endothelial cells synthesis various paracrine acting substances that influence vascular tone and permeability, coagulation and fibrinolysis, the composition of the subendothelial matrix, the adhesion and transmigration of leukocytes, and inflammatory activity in the vessel wall (10;21;22). Endothelial cells also interact with other cell types such as VSMC, platelets, and leukocytes (10).

Both insulin resistance and hyperglycaemia affect the development of endothelial dysfunction (23). Dysfunction of the endothelium is regarded as an important initial factor in the pathogenesis of atherosclerosis (10;22). Atherosclerosis is a progressive disease of large and medium-sized arteries, characterized by adherence of monocytes to the endothelium and diapedese and differentiation of monocytes to macrophages in

the tunica intima, uptake of oxidized low density lipoproteins (oxLDL) via scavenger receptors and transformation of macrophages to lipid rich foam cells that secrete proinflammatory cytokines and finally disrupts and thus contribute to lipid depositing and plaque formation (24;25).

1.2 Macromolecules function as signal molecules

The prevalence of people diagnosed with diabetes is estimated to rise considerably and is expected to include at least 366 million people in 2030 (26).

Type 2 diabetes accounts for around 90 % of all diabetes worldwide (27), and is a multifactorial disease with an environmental and genetic component. Excess nutrient intake plays a major role in the pathogenesis of the disease. Macromolecules like glucose, amino acids and fatty acids, function as signal molecules in nutrient sensing pathways. The hexosamine signalling pathway (HSP) is a nutrient signalling pathway activated by increased glucose flux (28), but is also sensitive to fluctuations in the concentration of free fatty acids, amino acids and the synthesis of nucleotides (29). Increased flux through the HSP is linked to insulin resistance. (30).

1.3 Hyperglycaemia increases metabolism through four metabolic pathways

The molecular mechanisms by which hyperglycaemia causes diabetic complications is not clear. In a cell susceptible for a hyperglycaemic environment, the intracellular glucose concentration is high and more glucose is metabolised via glycolysis and the tricarboxylic acid cycle (TCA), generating more electrons into the electron transport chain by NADH and FADH. The flux through the electron transport chain increases until a critical threshold occurs where the electron transfer inside the complex III is blocked. The surplus electrons are delivered to molecular oxygen, thereby generating superoxide (20). Superoxide inhibits the glycolytic enzyme glyceraldehyde-3 phosphate dehydrogenase (GAPDH) directing the glycolytic intermediates to four

different pathways; the polyol pathway, formation of advanced glycation end-product (AGE), activation of protein kinase C (PKC) and increased flux through the hexosamine pathway (Figure 1.1).

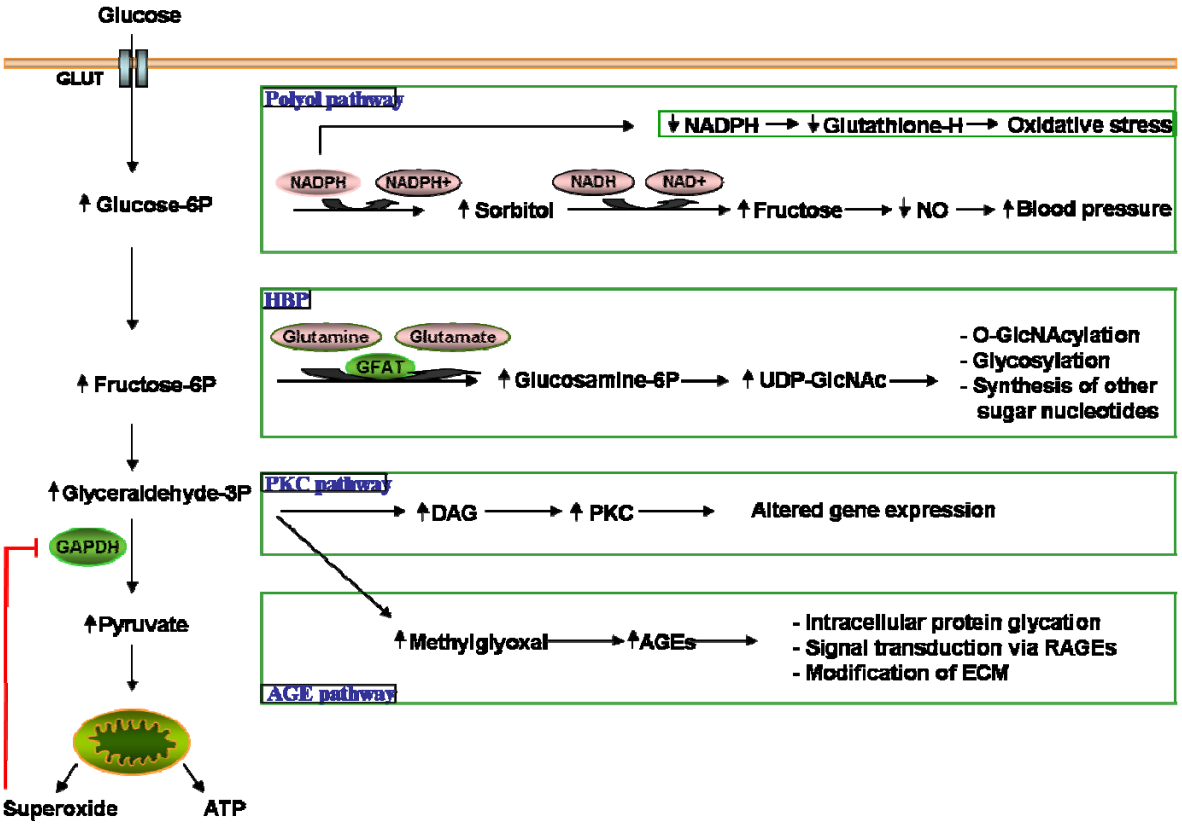

Figure 1.1. Hyperglycaemia activates four metabolic pathways, leading to cellular damage.

Hyperglycaemia induces overproduction of superoxide by the mitochondria. Superoxide inhibits the enzyme GAPDH, thereby generating more substrate for four different pathways; increased flux through the polyol pathway, increased formation of advanced glycation end-product (AGE), activation of protein kinase C (PKC) and increased flux through the hexosamine pathway. The figure is adapted from Brownlee. M. (19;20).

1.4 The hexosamine pathway

Glucose enters the cells via glucose transporters (GLUTs) and is subsequently phosphorylated to Glucose-6-phosphate by hexokinase (glucokinase in the liver). About 99 % of the intracellular glucose enters the glycolytic pathway or is converted to glycogen. 2-5 % of the glucose entering the cell is diverted into the hexosamine pathway (Figure 1.2) (31).

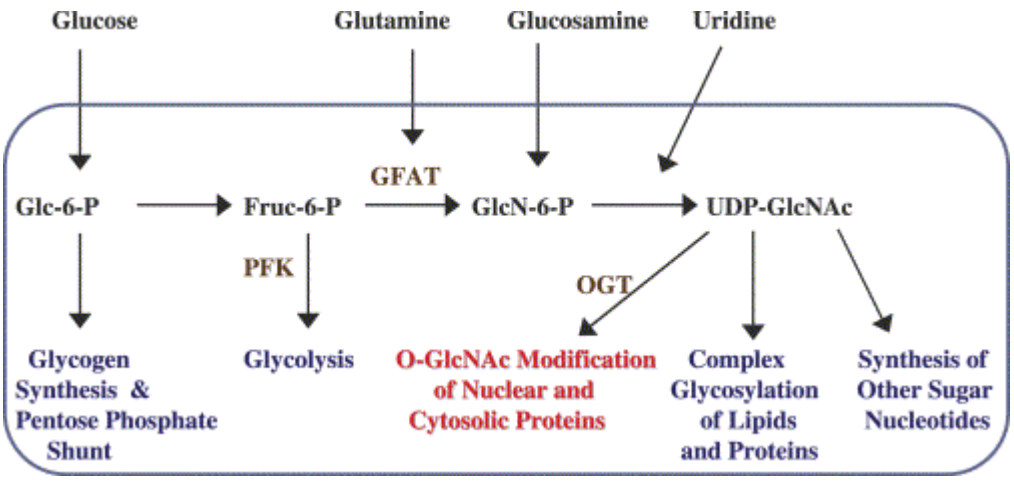

Figure 1.2. The hexosamine signalling pathway.

Fructose-6-phosphate is converted to glucosamine-6-phosphate by the rate limiting enzyme GFAT (L-glutamine:D-fructose-6-phosphate amidotransferase). UDP-GlcNAc is a building block for the formation of complex proteoglycans and glycoproteins in the secretory pathway and for O-GlcNAc modification of nucleocytoplasmic proteins (30;32). Figure from (33).

The rate limiting enzyme glutamine:fructose-6-phosphate amidotransferase (GFAT) catalyzes the formation of glucosamine-6-phosphate from fructose-6-phosphate and the aminodonor glutamine. GFAT is the rate limiting enzyme in the synthesis of glucosamine and is tightly regulated allosterically by UDP-GlcNAc and by PKA dependent phosphorylation (34;35). GFAT activity is found in almost every tissue examined (36), but the two gene products GFAT1 and GFAT2 have different tissue distribution patterns; GFAT1 is widely expressed, whereas GFAT2 is mainly

expressed in the central nervous system (36;37). GFAT1 activity is in contrast to GFAT2 activity increased by cAMP (PKA), indicating that different tissues metabolize glucose differently (36).

GFAT activity in adipocytes is down-regulated by insulin, glucose and glutamine (38). In myotubes, GFAT expression is increased by saturated fatty acids (39). GFAT is inhibited by the glutamine antagonists azaserine and 6-diazo-5 oxo-norleucine (DON) (40).

Glucosamine 6-phosphate is finally converted to UDP-GlcNAc. UDP-GlcNAc serves as a building block for the synthesis of proteoglycans and glycoproteins in the secretory pathway, and is also substrate for O-linked glycosylation (O-GlcNAcylation) of nucleocytoplasmic proteins (30).

1.5 O-GlcNAcylation and O-phosphorylation

O-GlcNAcylation is a dynamic posttranslational modification on intracellular proteins. O-GlcNAc consists of an O-linked attachment of a single N-acetylglucosamine on serine and threonine residues of nuclear and cytoplasmic proteins (Figure 1.3) (32;41). The conserved enzyme O-GlcNAc transferase (OGT) catalyzes the addition and O-GlcNAcase the removal of the O-GlcNAc (Figure 1.3). The modification is crucial for life and involved in signal transduction, translation, transcription and protein degradation (42).

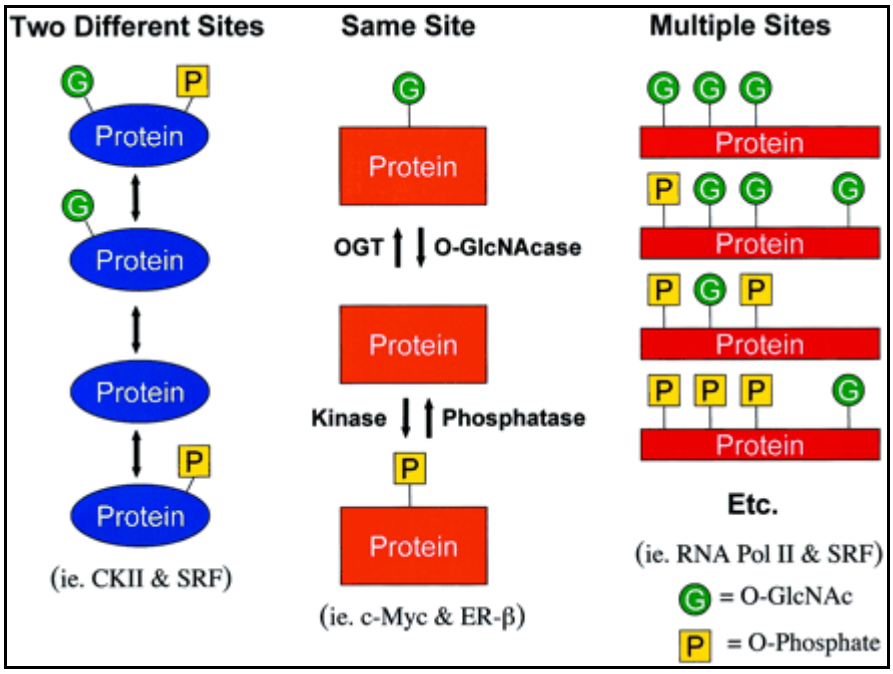

Figure 1.3. Dynamic interplay between O-GlcNAcylation and O-phosphorylation.

O-GlcNAc and O-phosphate share many common traits. Both O-GlcNAc and O-phosphate occurs on serine and threonine residues. The modifications can be found alone, they may compete for the same site, or several modifications can be found on the same protein. On some proteins O-GlcNAcylation and phosphorylation modify each other in a reciprocal manner. Figure from (43).

O-GlcNAcylation/de-O-GlcNAcylation is comparable with phosphorylation/de-phosphorylation (Figure 1.3). Like phosphorylation, O-GlcNAcylation is a dynamic posttranslational modification on intracellular proteins. Both modifications are found on serine or threonine in response to cellular signals, and the modified protein may have altered function. On some proteins, O-GlcNAc and O-phosphate compete for the same serine or threonine. The modifications may also be found on adjacent residues and may influence the other modification in a reciprocal manner. Several known phosphorylation sites are known O-GlcNAcylation sites, and multiple O-GlcNAcylation- and phosphorylation sites can be found on the same protein (31;43).

1.6 O-GlcNAc transferase (OGT)

O-GlcNAc transferase (OGT) is expressed in all tissues studied and OGT activity is essential for life (44). OGT is encoded by one gene, but alternative splicing generates three isoforms. The isoforms have different localization; ncOGT (nuclear/cytoplasmic), mOGT (mitochondrial), and sOGT (short OGT localized throughout the cell) (29).

The amount of O-GlcNAc modified proteins differ between subcellular compartments (31). Most O-GlcNAcylated proteins are found in the nuclear membrane, and listed in decreasing order: nuclei, rough microsomes, golgi, cytosol and mitochondria (29).

OGT is regulated by auto O-GlcNAcylation and tyrosine phosphorylation (Whelan, 2003, 1047) (29;31).

The OGT molecule consists of an N-terminal tetratricopeptide repeat (TPR) domain containing varying (1 - 16) number of TPR (34 amino acids repeats facilitating protein-protein interactions), and a C-terminal catalytic domain containing two conserved regions (CDI and CDII) **(Figure 1.4)** (45;46). Recently it was revealed that OGT interacts with a variety of phosphoinositides (PIPs) and it was discovered a PPO (PIP-binding activity of OGT) domain in the C-terminal (46).

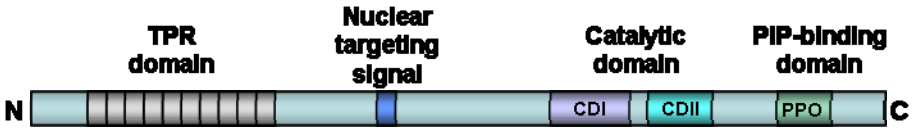

Figure 1.4. OGT primary structure.

The N-terminal domain contains varying number of TPRs. The C-terminal domain contains two conserved regions (CDI and CDII) (45). PPO is the recent identified PIP-binding domain (46).

In contrast to more than 500 kinases regulating phosphorylation, there is only one gene encoding OGT (41). It is not clear how one OGT molecule specifically can recognize a huge number of different target proteins, but it is suggested that the UDP-GlcNAc concentration, OGT protein-protein interactions, OGT phosphorylation and OGT glycosylation play a part (44).

1.7 O-GlcNAcase

O-GlcNAcase removes the O-GlcNAc from proteins and O-GlcNAcase is found in every human tissue examined (47). O-GlcNAcase (protein and activity) is localized primarily in the cytosol (90%), and 10 % is found in the nucleus (32). O-GlcNAcase is phosphorylated, and it is suggested that it also is regulated by interaction with other proteins (42;44). OGT and O-GlcNAcase have been found to sometimes occur in the same complex (31). O-GlcNAcase has at least two functional domains, a hexosaminidase domain and a histone acetyltransferase (HAT) domain (29).

Streptozotocin (STZ), PUGNAc (48) and NAG-thiazoline (49) are inhibitors of O-GlcNAcase. NAG-thiazoline is reported to act more potently than PUGNAc (49), but has not previously been used to study O-GlcNAcylation in HUVEC.

1.8 Functional consequences of O-GlcNAcylation

O-GlcNAc modifications have been identified on several proteins, including transcription factors, RNA polymerase II, kinases, phosphatases, metabolic enzymes, proteins in the cytoskeleton, nuclear pore proteins and signalling components (31;44;50). Dynamic O-GlcNAcylation is shown to be involved in regulation of protein phosphorylation, protein function, protein stability, localization of proteins, modulating protein-protein interactions and mediate transcription (44). It is reported that acute activation of protein O-GlcNAcylation is a stress response increasing cell survival during traumas or injuries (51). Dysregulated O-GlcNAcylation of proteins is associated with diseases, such as neurodegenerative diseases and cancer. Sustained

increase in O-GlcNAcylation has been associated with the pathogenesis of diabetes and diabetic complications (31;32). Increased level of O-GlcNAcylation has also been found in atherosclerotic plaque of diabetic patients (52).

1.9 O-GlcNAcylation in endothelial cells

Several O-GlcNAcylated proteins in human endotehlial cells are identified, mostly proteins in the insulin signalling cascade. Insulin modulates endothelial nitric oxide synthase (eNOS) activity and expression through the insulin receptor substrate-1 and-2 (IRS-1 and IRS2), phosphatidyl inositol 3-kinase (PI3K) and protein kinase B (Akt) signalling cascade. NO has vasodilatory effects, protects vessels from injury, inflammation and thrombosis, inhibits adherence of leukocytes to the endothelium, and reduces platelet aggregability and proliferation of smooth muscle cells (53). It has been shown that NO production is inhibited by hyperglycaemia induced O-GlcNAcylation on IRS1 and -2, p85 and eNOS (32;52), suggesting a role of O-GlcNAcylation in the pathogenesis of insulin resistance and diabetic complications.

1.10 Liver X receptor (LXR)

Liver X receptor (LXR)α and LXRβ constitute the nuclear receptor LXR subfamily. LXRβ is ubiquitously expressed, whereas LXRα is expressed mainly in the liver, adipose tissue and macrophages (54). LXR target genes have been shown to be involved in lipogenesis and cholesterol metabolism, glucose homeostasis, and inflammatory responses (54).

LXR have both favourable and unfavourable effects in diabetes. Favourable effects include suppression of proinflammatory cytokines, limitation of effects of glucocorticoids, inhibition of gluconeogenesis, lowering glucose levels in serum and induction of reverse cholesterol transport. Unfavourable effects include induction of fatty acid production and increased triacylglycerols in serum (54).

LXR have mostly been studied in liver, adipose tissue and muscle, but the effect of LXR in endothelial cells has not been extensively examined. ABCA-1 is an LXR target gene involved in reverse cholesterol transport, stimulating cholesterol efflux to apolipoproteins. Low density lipoproteins (LDL) is shown to activate LXR and induce up-regulation of ABCA-1 expression in endothelial cells (55), whereas oxidized low density lipoproteins (oxLDL) inhibits activation of LXR and down-regulates ABCA-1 expression. OxLDL induced down-regulation of ABCA-1 may contribute to endothelial dysfunction and plaque formation (56).

LXR function as a heterodimer with retinoid X receptor (RXR) (Figure 1.5). The LXR-RXR heterodimer is bound to LXR response element (LXRE) in the promoter of target genes in complex with corepressors. Upon ligand activation, the heterodimer undergoes a conformational change that induces the release of the corepressors and recruits coactivators and increase transcription of the LXR target genes. The LXR-RXR complex acts as a nutrient sensor (57) activated by either LXR ligands, RXR ligands or synergistically by ligands of both receptors (57;58).

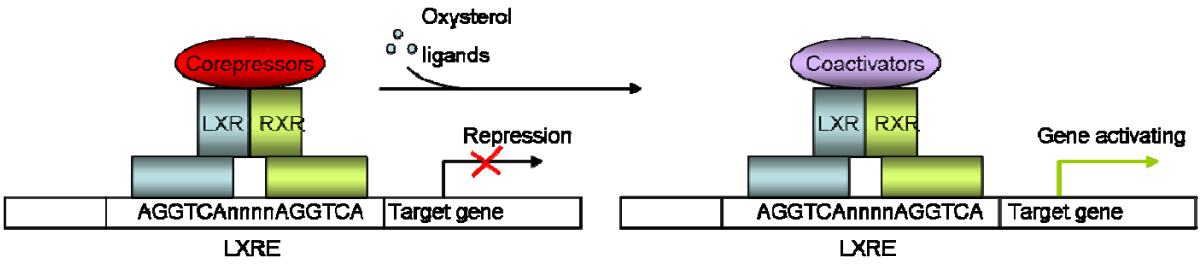

Figure 1.5. LXR

Liver X receptors (LXRs) are cholesterol sensing transcription factors. In the nucleus, LXR-retinoid X receptor (RXR) heterodimers are bound to LXR response elements (LXREs) in the promoter of target genes with corepressors. Upon ligand binding, the corepressors are exchanged for coactivator complexes and transcription of target gene is induced. Figure adapted from (59).

Oxygenated derivatives of cholesterol (oxysterols) are natural LXR ligands which bind to a hydrophobic pocket in the C terminal domain and activate gene transcription of LXR target genes. Recently, it was suggested that glucose binds and

regulates LXRα and -β in the liver. Glucose was more potent on LXRβ than LXRα (60). However, the hydrophilic nature of the glucose molecule suggests that glucose rather acts via downstream glucose signalling pathways, potentially via hexosamine signalling pathway and O-GlcNAcylation of LXR. We performed a search for potential O-GlcNAcylated sites on LXR using the YinOYang prediction program (1), revealing that LXRα (Appendix A) and LXRβ (Appendix A) have several potential O-GlcNAcylation sites.

1.11 Inhibitors of DNA binding and differentiation (Id proteins)

Id (inhibitors of DNA binding and differentiation) family of proteins consists of four gene products (Id1-Id4) of similar size (13-20 kDa) (61). Id1 and Id3 have different splice variant (62;63).

The level of Id expression varies among different tissues, and is generally low in un-proliferating and differentiated cells (64;65). Id1 and Id3 are nearly ubiquitously expressed, whereas Id2 is mainly expressed in bone marrow, testis and brain, and Id4 in testis, brain and kidney (65;66). Id1, Id2 and Id3 are expressed in endothelial cells during embryogenesis, however at birth Id genes are down regulated in most mature tissues (67). Id3 protein is expressed at low levels in normal vessels, whereas Id2 is normally absent from the vessel wall (64).

The Id family belongs to the helix-loop-helix (HLH) family of transcription factors (61;64;68;69). The primary targets for the Id proteins are the basic HLH (bHLH) transcription factors (61;64;68;69). Basic HLH transcription factors forms homo- and heterodimers that bind DNA sequences termed E-boxes in the promoter region of target genes and activate transcription (Figure 1.6). The Id proteins lack the basic DNA binding region and form inactive heterodimers with class I of bHLH proteins (Figure 1.6).

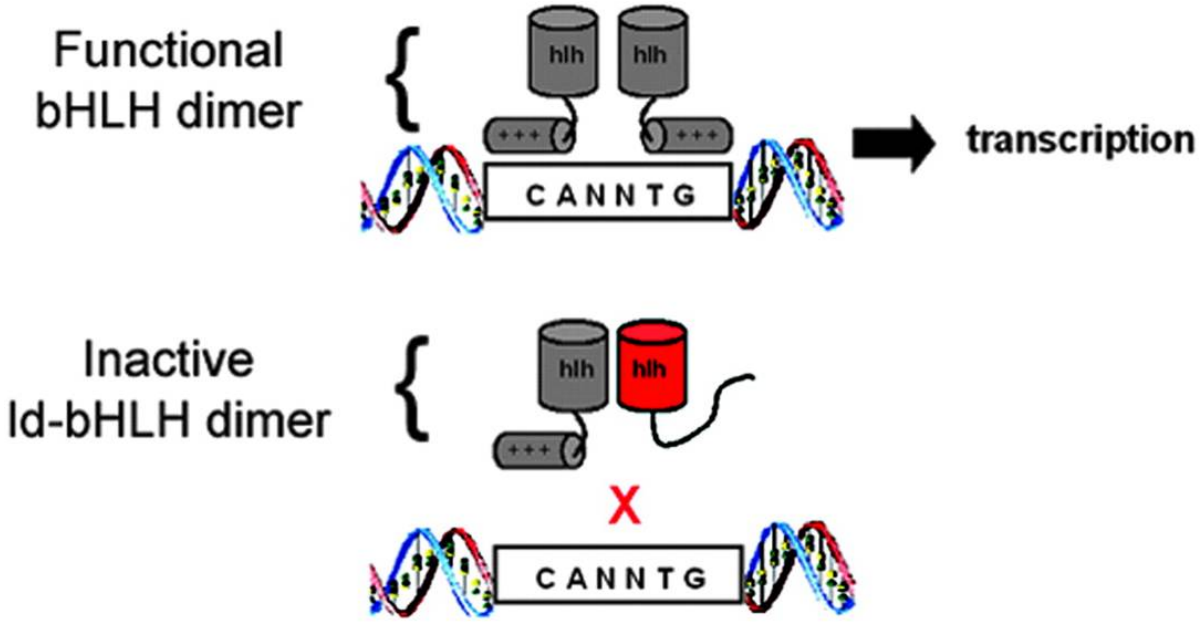

Figure 1.6. The Id proteins act as dominant-negative regulators of transcription.

Primary targets for Id proteins are the basic helix-loop-helix (bHLH) transcription factors. The HLH-region of bHLH mediates dimerization, and the basic region is responsible for specifically binding DNA sequences termed E-boxes (61). Id proteins lack the basic region necessary for binding to DNA, and dimers with Id proteins are thus unable to activate gene transcription. Figure from (64).

Class II of bHLH proteins are incapable of forming homodimers (with few exceptions), and normally form heterodimers with class I proteins. Id proteins thus also regulate class II proteins by heterodimerize with class I proteins and prevent them from forming heterodimers with class II proteins (61;64;65). Id proteins are also shown to dimerize with other bHLH proteins such as SREBP (class III) and proteins that do not contain an HLH domain, for example the cell cycle regulator retinoblastoma protein (Rb) (64;70).

The Id proteins regulates several cellular processes, including transcription of cell cycle genes, differentiation, haematopoiesis, angiogenesis, neurogenesis, myogenesis, and developmental processes (64;67;68). Id expression levels are increased in atherosclerosis, inflammation (65) and cancer (69).

Dysregulated angiogenesis, the formation of new blood vessels out of pre-existing capillaries, is a characteristic of diabetes. Impaired angiogenesis may lead to reduced wound healing in peripheral limbs and reduced collateral development of cardiac vessels contributing to diabetic ischemia and increased cardiac mortality. However, angiogenesis into an atherosclerotic plaque is associated with increased risk of intra plaque haemorrhages, plaque rupture and fatal outcome. Diabetic patients have increased risk for intra plaque haemorrhage (71). Enhanced angiogenesis have also been observed in the retina, contributing to diabetic retinopathy (72).

Id proteins play a major role in angiogenesis (73). It is shown that overexpression of Id can induce angiogenic processes in HUVEC (transmigration, expression of matrix metalloproteinases-2 and -9, and tube formation) (74). Id proteins are thought to facilitate angiogenesis in tumours (67), and there are similarities between angiogenesis in tumours and angiogenesis into plaques (69).

The effects of hyperglycaemia on angiogenesis are not fully understood. Hyperglycaemia is reported to inhibit angiogenic processes in HUVEC (72) and it was recently reported that increased level of glucosamine induced O-GlcNAc modifications in endothelial cells may contribute to dysregulated angiogenesis (72).

It is shown that Id1 protein is up-regulated by glucose in pancreatic β-cells (70), and previous studies in our group have shown that Id2 is up-regulated by hyperglycaemia in murine J774.2 macrophages via the hexosamine signalling pathway (75). Preliminary experiments in our laboratory also indicate that Id2 is target for O-GlcNAcylation (76). It is not known whether Id protein expression in HUVEC is regulated by D-glucose, or whether they are targets for O-GlcNAcylation.

1.12 Aim of study

The objective of this study was to identify hyperglycaemia induced O-GlcNAcylated proteins in primary human endothelial cells with the aim of elucidate their role in endothelial dysfunction with specific focus on the transcription factors Id proteins and LXR.

Specific aims:

- Test the effect of the O-GlcNAcase inhibitor NAG-thiazoline on protein O-GlcNAcylation in HUVEC.
- Study the effect of hyperglycaemia on the total level of O-GlcNAcylated proteins in HUVEC
- Study whether D-glucose regulates Id protein expression and whether they are targets of O-GlcNAcylation in HUVEC
- Study whether LXR is a target of O-GlcNAcylation in HUVEC

2. Methods

Materials

Amersham Hyperfilm™ ECL	GE Healthcare, UK
Bűrker Haemacytomer	Marlenfield, Germany
Cell culture plastic plates (6 wells)	BD Labware, USA
Cell scraper	Sigma Aldrich, Germany
Criterion™ gel system	Bio-Rad, USA
Criterion Precast gel (4-20 %), 18 wells	Bio-Rad, USA
Criterion Precast gel (4-20 %), 12 wells	Bio-Rad, USA
Criterion Precast gel (12+ %)	Bio-Rad, USA
Criterion Precast gel (7.5 %)	Bio-Rad, USA
Criterion Precast gel (10 %), 18 wells	Bio-Rad, USA
Criterion Precast gel (10 %), 12 wells	Bio-Rad, USA
ELISA microplate (96 well)	Greiner bio-one, Germany
Eppendorf tubes (1.5 ml)	Sarstedt, Germany
Falcon tubes (5 ml, 15 ml)	BD Labware, USA
Hypercassette™ autoradiography cassettes	Amersham, UK
Immobilon™ Transfer Membrane (PVDF)	Millipore, USA
Mesoft compresses	Tendra, Sweden
Metal cannulas	Technical Department, UIO
Omnifix® single use syringes (10 ml, 50 ml)	Braun, Germany
Pipetboy	INTEGRA Biosciences AG, Switzerland
Single use scalpel	Paragon®, UK
Sterican sterile needle	Regent, USA
Sterile cell culture flasks (25, 75, 150 cm^2)	BD Labware, USA

Sterile filter flasks	TPP, Switzerland
Sterile surgical gloves with biogel coating	Regent, USA
Stripettes (5 ml, 10 ml, 25 ml)	BD Labware, Germany
Whatman® filter paper	Schleicher & Schuell

Instruments

Celloshaker variospeed	Vialta, Italy
Centrifuge Kubota 5930	Kubota, Japan
Centrifuge 5417 R	Eppendorf, Germany
Dri Block Heater	Total Lab Systems Ltd, New Zealand
Kodak X-OMAT, 1000 Processor	Kodak
Incubator Forma	Scientific Incorporation, USA
Mettler Toledo Model AX105DR Delta Range Scale®	Mettler, Norway
Microscope Olympus (CKX 415F)	Olympus Corp., Japan
pH-meter: PHM210	MeterLab®, France
Titertek Multiskan PLUS	Eflab, Finland
Rotating device: Ld-76	Labinco B.V. The Netherlands

Chemicals

4-(2-Aminoethyl) benzenesulfonyl fluoride hydrochloride (AEBSF)	Calbiochem®, USA
ALLN	Calbiochem®, USA
BC Assay protein quantification kit	Uptima Interchim, France
β-mercaptoethanol (C2H6OS)	Sigma-Aldrich, Norway

Bovine serum albumin (BSA)	Sigma Aldrich, Germany
Bromphenol blue	Bio-Rad, USA
Collagenase (0.2 %)	Sigma Aldrich, Germany
Coomassie Brilliant Blue (G)	Sigma Aldrich, Germany
Complete Mini EDTA-free Protease inhibitor cocktail tablets	Roche, Germany
D(+)-Glucose	Sigma Aldrich, Germany
Dithiothreitol (DTT)	Fermentas, Sweden
ECL™ Western blotting detection reagent	Amersham, UK
ECL™ Plus Western blotting detection reagent	Amersham, UK
Ethylenediaminetetraacetic acid (EDTA)	Sigma-Aldrich, Germany
Epidermal growth factor (EGF)	R&D systems, UK
Foetalt bovine serum (FBS)	Sigma Aldrich, Germany
Fibroblast growth factor (FGF)	R&D systems, UK
Fungisone	GIBCO Invitrogen, UK
Glycerol	Sigma-Aldrich , Germany
Glycine	Sigma-Aldrich, Germany
Hydrocortisone	Sigma Aldrich, Germany
Hydrogen chloride (HCl)	Merck, Germany
Igepal CA-630 (NP-40)	Sigma-Aldrich
Insulin Actrapid® Penfil®	Novo Nordisk A/S, Denmark
KH_2PO_4	Merck, Germany
Magnesium chloride ($MgCl_2$)	Merck, Germany
MCDB131 basis powder	Sigma Aldrich, USA M8537-1L
Methanol	Merck, Germany
N-acetylglucosamine (Chitin hydrolysates)	Vector Laboratories, UK
NAG-thiazoline	Gift from Dr. Spencer Knapp (49)
NaH_2PO_4 x $2H_2O$	Merck, Germany

Precision Plus Protein Standards (All blue)	Bio-Rad, USA
Precision Plus Protein Standards (Dual color)	Bio-Rad, USA
RPMI 1640 with L-glutamin, without glucose	Gibco Invitrogen, UK
Sodium dodecyl sulphate (SDS)	Sigma-Aldrich, Norway
Sodium chloride (NaCl)	Merck, Germany
Sodium fluoride (NaF)	Sigma Aldrich, Norway
Sodium hydrogen carbonates ($NaHCO_3$)	Merck, Germany
Sodium Hydroxide (NaOH)	Merck, Germany
Sodium orthovanadate (N_3VO_4)	Sigma-Aldrich, Germany
Sodium pyrophosphate (NaPPi)	Sigma Aldrich, Germany
Tris Base	Calbiochem, USA
Trypan blue solution	Sigma-Aldrich, UK
Trypsin-EDTA Solution (1x)	Sigma-Aldrich, Norway
Tween® 20	Sigma Aldrich, Germany

Tissues

Human umbilical cords	Rikshospitalet, Oslo

Antibodies

Id1 (C-20) Rabbit polyclonal IgG antibody	Santa Cruz Biotechnology, Santa Cruz, Sc-488
Id2 (C-20) rabbit polyclonal IgG antibody	Santa Cruz Biotechnology, Santa Cruz, Sc-489
Id3 (C-20) rabbit polyclonal IgG antibody	Santa Cruz Biotechnology, Santa Cruz, Sc-490

CTD 110. 6 monoclonal antibody	Covance, UK, MMS-248R
RL-2 mouse monoclonal antibody	ABR Affinity BioReagents^{TM}, USA, Cat.No: MA1-072
LXR α/β (R20) goat polyclonal IgG antibody	Santa Cruz Biotechnology, Santa Cruz, SC-1206
Mouse Anti-Human LXR beta / NR1H2 IgG2a, Monoclonal Antibody	R&D, Cat. No: PP-K8917-10
β-Actin (C4) mouse monoclonal antibody	Santa Cruz Biotechnology, Santa Cruz, SC-47778
Goat Anti-Rabbit IgG secondary antibody	Jackson immuno Research, USA, Cat. No: 111-035-144
Goat Anti-Mouse IgG secondary antibody	Jackson immuno Research, USA, Cat. No: 115-035-146
Goat Anti-Mouse IgG secondary antibody, light chain	Jackson immuno Research, USA, Cat. No: 115-035-174
Mouse Gamma Globulin	Jackson Immuno Research, USA, Cat. No: 015-000-002
Rabbit Gamma Globulin	Jackson Immuno Research, USA, Cat. No: 011-000-002
Goat Anti-Mouse IgM secondary antibody	Sigma-Aldrich Co, USA, Cat. No: A 8786
Rabbit Anti-Goat IgG secondary antibody	Southern Biotech, USA Cat. No: 6160-05
OGT (AL28)	Gift from Dr. Hart (2003) (77)

2.1 Complete MCDB-medium

Procedure

The MCDB-powder was transferred to a glass vial containing 850 ml MilliQ-H_2O and stirred until dissolved. While stirring, 1.18 g sodium hydrogen carbonates ($NaHCO_3$) was added, and the pH was adjusted to 7.3. The final volume was adjusted to 1000 ml by adding MilliQ-H_2O. The medium was sterile filtered through a sterile filter flask with a 0.22 microns membrane. The medium was made complete by adding sterile epidermal growth factor (EGF) (500 µl), 50 µl fibroblast growth factor (FGF), 500 µl gentamicin, 50 µl hydrocortisone, 500 µl fungisone and 7% heat inactivated foetal bovine serum (FBS) (table 1).

2.2 Isolation of Human Umbilical Vein Endothelial Cells (HUVEC)

The inside surface of blood vessels are formed by a single layer of endothelial cells. Human Umbilical Vein Endothelial Cells (HUVEC) are primary endothelial cells isolated from human umbilical cord vein and were first successfully cultured in vitro by Jaffe and Nachman in 1973 (78). HUVEC were obtained from the obstetric and gynaecology division, Rikshospitalet, Oslo from healthy mothers with normal pregnancies. Written consent was obtained from the mothers and ethical approval was obtained from the Human Research Ethical Committee (79).

Procedure

HUVEC were isolated from human umbilical cord veins by an adaptation of the method of Jaffe et al (78). A sterile technique was utilized in all operations of the cord. The cord was placed in a container filled with transporting buffer (Table 2) immediately after delivery and stored in the fridge (4^oC) for maximum 48 hours. The

umbilical vein was cannulated with a metal cannula and a 50 ml sterile syringe was coupled to the cannula via a 2-3 cm plastic tube. The vein was perfused with 1x PBS (Table 3) to wash out the remaining blood. The other end of the vein was cannulated and coupled to a 10 ml syringe and 10 ml of 0.2 % collagenase in 1x PBS was infused. The cord containing the 0.2 % collagenase was placed in a glass vial filled with sterile 1x PBS at 37^{o}C for 10 minutes, allowing the endothelial cells to separate from the vein wall followed by centrifugation for 10 minutes 470 x g. The cell pellet was resuspended in 5 ml complete MCDB131-medium, and the cells were transferred to a 25 cm^2 cell culture flask and incubated at 37^{o}C in a humidified 5 % CO_2 atmosphere. The culture medium was changed the next day to remove blood cells.

2.3 Culturing and splitting of HUVEC

The HUVEC were cultured in 25 cm^2 cell culture flasks (5 ml pr. flask), 75 cm^2 cell culture flasks (15 ml pr. flask), or 150 cm^2 cell culture flasks (25 ml pr. flask). The cells were seeded into 6-well plates (2 ml pr. well) during experiments. The cells were fed 3 times a week with a complete change of culture medium. At 80 -100 % confluence, the cells were split at a 1:3 ratio. Cells from passages 2-4 were used in all experiments. Cells from later passages may have changes in phenotype, and it is advised to discard cells beyond the 6th passage (80).

Endothelial cells adhere to the extracellular matrix and neighbouring cells via adhesion molecules. There are both calcium dependent and calcium independent mechanisms of cell adhesion. Trypsin is a proteolytic enzyme of the serine protease family and Ethylenediaminetetraacetic acid (EDTA) is a metal ions chelator which removes Ca^{2+} ions. Trypsin-EDTA can disrupt both cell-cell and cell-matrix interactions, and Trypsin-EDTA solution was used to remove adherent cells from the culture surface.

Procedure

Old medium was removed by aspiration, and the cells were washed with 2 ml Trypsin-EDTA (1x) solution (2 ml to 25 cm^2 culture flask). Trypsin-EDTA (3 ml) was added, and the culture flask was incubated at 37^oC for 5-6 minutes. The detached cells were visualized in microscope as round shaped cells. Complete medium (5 ml) containing 7 % FBS was added in order to inhibit further tryptic activity which may damage the cells. Calcium and proteins in FBS inhibit Trypsin and Trypsin-like activities. After centrifugation at 1500 rotations per minute (rpm), the cell pellet was resuspended in complete MCDB131- medium, transferred to 25 cm^2, 75 cm^2 or 150 cm^2 cell culture flasks, and incubated at 37^oC, 5 % CO_2.

2.4 Lysis of cells

RIPA (Radio-Immunoprecipitation Assay) buffer is used for whole cell lysis and is useful when studying total protein level. As soon as lysis occurs, proteolysis, deglycosylation, phosphorylation/dephosphorylation and denaturation begin. These processes can be slowed down if the samples are kept at 4°C and appropriate inhibitors are added fresh to the lysis buffer. In order to avoid deglycosylation after lysis, we added NAG-thiazoline, an inhibitor of O-GlcNAcase (49).

Procedure

The cells were grown in 6 well plates and stimulated at 80-100 % confluence. The MCDB131 medium was replaced with RPMI 1640 medium containing 7 % FBS and 1 mM D-glucose, without supplements over night. The next day, the cells were incubated with various concentrations of NAG-thiazoline or D-glucose as specified in the figure legends. All further procedures were performed on ice in order to slow down proteolysis. After removing the media by aspiration, the cells were washed two times with ice-cold 1x PBS, 1 ml per well. 250 µl Ice-cold RIPA-buffer (Table 4) were added pr. well, and the cells were scraped with a cell scraper. The extract was then transferred to eppendorf tubes, left on ice for 30 minutes and flicked at intervals to dissolve material. The extract was centrifuged 14 000 rpm for 10 minutes at 4^oC

and the supernatant was transferred to clean eppendorf tubes. The protein concentration was measured, and the concentration was adjusted to the same protein concentration with RIPA-buffer. The lysates were stored at -80^{o}C or mixed with loading dye (2x) (Table 5), boiled for 5 minutes and stored at -20^{o}C until SDS-PAGE and western blotting.

2.5 Preparation of nuclear and cytoplasmic extracts

Proteins that are found predominantly in the nucleus can be enriched in a nuclear lysate. A nuclear protein will constitute a larger proportion of the total protein in a nuclear lysate than in a whole-cell lysate, making it easier to obtain a signal from a weakly expressed protein.

Procedure

The cells were grown in 6 well plates and stimulated at 80-100 % confluence. All procedures were performed on ice.

After removing the media by aspiration the cells were washed two times with ice-cold 1x PBS (0.5 ml per well). Ice-cold lysis buffer (250 µl) (Table 6) were added pr. well, and the cells were scraped with a cell scraper. The cells were transferred to a glassgrinder and lysed by moving the pestle up and down ten times. After spinning at 3500 rpm for 10 minutes at 4^{o}C, the supernatant, which now constituted the cytoplasmic extract, were transferred to eppendorf tubes. The nuclear pellets were resuspended in 1x PBS. To confirm the presence of nuclei, 40 µl of the resuspended pellet were removed and mixed with 40 µl trypan blue. Blue, round shaped nuclei were visualized with a light microscope. After centrifugation at 3500 rpm for 10 minutes at 4^{o}C, the nuclear pellets were resuspended in 100 µl ice cold NE2 lysis buffer (Table 7) and left on ice for 30 minutes. The tubes were flicked approximately every 10th minutes. The nuclear extracts were diluted to 520 µl with lysis buffer (1x PBS containing 0.2 % NP-40) and 20 µl was removed for measuring protein concentrations.

2.6 Measurement of protein concentration

The BCA Protein Assay was used to determine the protein concentration of the cell lysates. In an alkaline environment proteins will reduce Cu^{2+} to Cu^{1+}. In the BCA assay, this property is combined with a colorimetric detection of Cu^{1+} by bicinchoninic acid (BCA). The amount of Cu^{2+} reduced is proportional to the amount of protein present in the solution.

Procedure

Different concentrations of BSA (2 mg/ml stock solution) were used to prepare a standard curve. MQ-H_2O, BSA and lysis buffer were added to a 96-well plate as shown in Table 8. Lysis buffer was added to each standard in the same amount as the samples in order to correct for possible buffer effects. The standards were made in duplicates.

Each sample was prepared in triplicates by adding 5 µl of the sample and 45 µl MQ-H_2O to the 96-wells plate. Protein assay reagent A and protein assay reagent B were mixed 50:1, and 200 µl of the A + B solution was added to each well. The 96-wells plate was incubated at 37^{o}C for 30 minutes before the absorbance was measured at 562 nm. The absorbance of the BSA standards (y-axis) was plotted against the known BSA concentrations (x-axis) and the protein concentration of the samples was determined.

2.7 Immunoprecipitation (IP)

Immunoprecipitation (IP) is a method by which a protein can be isolated from a protein lysate using an antibody specific to the protein of interest. The protein bound antibody is then pelleted out of solution by centrifugation following incubation with protein A/G agarose beads.

Procedure

Nuclear- or whole-cell lysates were prepared as described. The specific antibody was added to the cell lysate and left over night at 4°C on a rotating device. A control sample was prepared by adding gamma globulin of the same species in the same concentration as the antibody and left over night at 4°C on a rotating device. The next morning, both the sample and the control sample were incubated with 25 µl Protein A/G PLUS-Agarose beads at 4°C for 1 hour on a rotating device followed by centrifugation at 2500 rpm for 1 minute at 4°C. Supernatants (post-IP lysates) were transferred to clean eppendorf tubes. The pellets were washed 3 times in lysis buffer in order to remove unspecific proteins. The pellets were resuspended in 100 µl 2x loading dye, 50 µl post-IP lysate was mixed with 50 µl 2x loading dye, and 50 µl pre-IP lysate (input control) was mixed with 50 µl 2x loading dye. The samples were boiled for 5 minutes and 30 µl was further analyzed by SDS-PAGE and western blotting.

2.8 Precipitation of N- and O-GlcNAcylated proteins

Succinylated wheat germ agglutinin (sWGA) is a lectin that specifically binds terminal O- and N-GlcNAc and is used to precipitate O-and N-GlcNAcylated proteins.

Procedure

In order to remove agarose binding proteins, lysate (500 µl) was incubated with 25 µl Protein A/G PLUS-Agarose beads and incubated at 4°C on a rotating device for 45 minutes - 1 hour. After centrifugation at 2500 rpm for 1 minute at 4°C, the supernatant was transferred to clean eppendorf tubes. The sWGA was washed 3 times in lysis buffer and lysates were incubated with 40 µl sWGA (1:1 v/v slurry) at 4°C on a rotating device over night. The next day, the samples were centrifuged 1 minute at 2500 rpm, 4°C, and the sWGA pellets washed 3 times in lysis buffer. The post-sWGA lysate (50 µl) was transferred to clean eppendorf tubes and mixed with 50 µl 2x loading dye. The sWGA pellets were resuspended in 100 µl 2x loading dye. Pre-

precipitation lysates (50 µl) were mixed with 50 µl 2x loading buffer. All the samples were boiled for 5 minutes in a heating block before SDS-PAGE and western blotting, or stored at -20^{o}C.

2.9 SDS-PAGE (Sodium dodecyl sulphate-Polyacrylamid gel electrophoresis)

Polyacrylamide gel electrophoresis (PAGE) is the migration of proteins through pores in a polyacrylamide gel matrix in response to an electrical field.

Sodium dodecyl sulphate (SDS) is an anionic detergent which denature the proteins (i.e. disrupts the secondary, tertiary and quaternary structure of the proteins) together with β-mercaptoethanol and heating. The proteins bind about 1.4 g SDS/g protein, and SDS will coat the proteins with negative charges in proportion to their length, allowing the proteins to migrate towards the anode.

The polyacrylamide gel is formed from the polymerization of acrylamide monomers in the presence of smaller amounts of the crosslinking agent N,N´-methylene-bis-acrylamide. When the polymer is formed, it turns into a gel with different pore sizes according to the concentration of the acrylamide. Gels with high concentration of acrylamide will have smaller pore size than gels with low acrylamide concentration. The smaller molecules are able to navigate the smaller pore size more easily than the larger molecules, and the proteins are thus separated according to size.

Procedure

The cell lysates and IPs were prepared and mixed with 2x loading dye as described above and boiled for 5 minutes before loading. The electrophoresis apparatus and pre-cast gel was assembled according to manufactures instructions (Bio-Rad). Running buffer (Table 9) was poured into the container, and equal amounts of protein were loaded into each well. Protein standards were loaded to marginal wells on both sides. The SDS-PAGE was run at 120-150 V until the bromphenol blue and protein standards reached the bottom of the gel.

2.10 Western blotting

In western blotting assays, an antibody is used to identify a specific protein of interest or a post-translational modification (i.e. O-linked glycosylation, phosphorylation) of an immunoprecipitated protein or proteins in a lysate separated on the gel. First, the SDS-PAGE separated proteins must be transferred from the polyacrylamide gel to an Immobilon-Polyvinylidene fluoride (PVDF) membrane by an electric currant in order to make the proteins accessible to antibody detection. The proteins maintain the same relative position they had in the gel. For enhanced chemiluminescence (ECL) detection, the primary antibody is incubated with a secondary antibody conjugated to the enzyme horseradish peroxidase (HRP). In the presence of hydrogen peroxide, HRP converts luminol to dianion, an excited intermediate which emits light (luminescence) when it returns to its ground state. The light produced is in proportion to the amount of protein. The light can be captured on a sensitive film. The size of the protein can be determined relative to a size marker standard and the protein quantity can be determined relative to the intensity of other bands.

Procedure

For each gel, one PVDF membrane and four filter papers were cut in the same size as the gel. The PVDF membrane was soaked in methanol in order to be compatible with aqueous systems. The membrane was rinsed in MQ-H_2O and equilibrated in transfer buffer (Table 10). Two fiber pads and the filter papers were dipped in transfer buffer before the assembly of the cassette. The cassette was assembled in following order: red side of the cassette, 1 fiber pad, 2 filter papers, PVDF membrane, gel, 2 filter papers, and 1 fiber pad. The red side of the cassette was inserted into the red side/anode of the blotting apparatus to allow the negatively charged proteins in the gel transfer to the membrane. One cooling block and a stirring bar were placed into the container and the container was filled with transfer buffer. The blotting apparatus was placed on a magnetic stirrer and transfer conducted at 100 V for 60 minutes. The cooling block was replaced after 30 minutes in order to avoid over heating.

To avoid unspecific binding, the PVDF membrane was blocked in 3 % BSA-TBST for 45-60 minutes. The membrane was thereafter transferred to a 50 ml Falcon tube and incubated with the primary antibody diluted in 3 % BSA-TBST at 4^{o}C over night on a rolling device. The next day, the membrane was washed 3 x 5 minutes in TBST to remove unbound antibody before the membrane was incubated with a HRP-conjugated secondary antibody diluted in 3 % BSA-TBST for 45 minutes on a shaker at room temperature. Next, the membrane was washed twice in MQ-H_2O and incubated with an ECL solution containing the substrates for HRP. The membrane was then placed in a Hypercassette™, the light produced was captured on a film and the image developed in a film developer machine. Molecular weight markers were used to determine the size of the proteins.

2.11 Stripping the PVDF membrane

The PVDF membrane can be stripped for both primary and secondary antibodies and be reprobed with new antibodies.

Procedure

The membrane was incubated at 50^{o}C for 30 minutes in stripping buffer (Table 11) while rotating. The membrane was washed 3 x 5 minutes in TBST (Table 12) and reblocked in 3% BSA-TBST for 1 hour at room temperature before reprobing with primary- and secondary antibodies as described.

3. Results

3.1 Concentration and time dependent effects of NAG-thiazoline on protein O-GlcNAcylation in HUVEC

NAG-thiazoline is reported to be a more potent inhibitor of O-GlcNAcase than PUGNAc (49), but has not to date been used to study O-GlcNAcylation in HUVEC. NAG-thiazoline is not yet commercially available, and was kindly provided by Dr. Spencer Knapp (49).

To test the dose needed for this inhibitor to increase protein O-GlcNAcylation in HUVEC, a dose-response experiment with different NAG concentrations were performed. 10 μM NAG-thiazoline was sufficient to induce an increase in overall O-GlcNAcylation in HUVEC as shown in Figure 3.1A. This is 10 times more potent than the optimal PUGNAc concentration used to study O-GlcNAcylation (46;81-84).

Immunoblot intensities of bands of approximately 55 and 60 kDa were strongest in cells incubated with 10 μM NAG-thiazoline compared to 0, 20 and 40 μM (Figure 3.1A). No further effect of NAG-thiazoline on O-GlcNAcylation was observed in cells treated with concentrations above 10 μM (Figure 1A).

The difference in total O-GlcNAcylation levels between the samples from cells treated with or without 10 μM NAG were apparent two hours after incubation (Figure 3.1B), but the total level of O-GlcNAcylated proteins were highest 24 hours after incubation. The size of the NAG induced O-GlcNAc immunoreactive bands were approximately 55, 60, 80, 90, 145, 155, 250 kDa.

The general O-GlcNAc antibodies CTD 110.6 and RL2 detect subsets of O-GlcNAcylated proteins giving a view of the overall O-GlcNAcylation, but do not detect all possible O-GlcNAcylated proteins. Both antibodies preferentially recognize high molecular weight proteins. CTD 110.6 was used in the immunoblot experiments

in figure 1. We also performed parallel blots using RL2 which detected a similar pattern of immunoreacitve bands (data not shown).

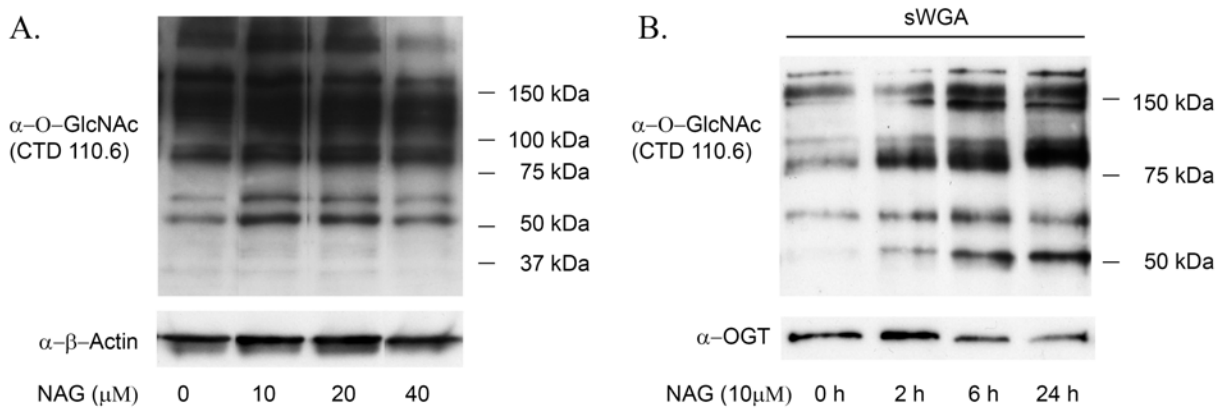

Fig. 3.1. Concentration and time dependent effects of NAG-thiazoline on O-GlcNAcylation in HUVEC

A. HUVEC were treated with 0, 10, 20 and 40 µM NAG for 24 hours. Whole cell extract was prepared and 22 µg protein pr. lane was separated by SDS-PAGE (4-20 % gel) followed by western blotting using the monoclonal antibody CTD 110.6 which detects a subset of O-GlcNAcylated proteins. β-Actin was used as a loading control. **B.** HUVEC were incubated with 10 µM NAG for 2, 6 and 24 hours. Whole cell extract was prepared and the protein concentration was adjusted to 0.9 µg/µl, before N-and O-GlcNAcylated proteins were precipitated from 500 µl lysate using sWGA. The same amount of samples were loaded in each lane and analyzed by SDS-PAGE (4-20 % gel) and western blotting using CTD 110.6. The antibody OGT was included as a positive control.

3.2 Effects of glucose on the level of protein O-GlcNAcylation in HUVEC

To examine the time-effects of hyperglycaemia on the general level of O-GlcNAcylated proteins in HUVEC, cells were grown in 5 or 25 mM D-glucose and harvested 4, 24, 48 and 72 hours after incubation. The media was changed every 24

hour to avoid secondary autocrine effects of hyperglycaemia and to maintain the glucose concentration. Whole cell lysates were analyzed by immunoblotting.

The total level of O-GlcNAcylation increased with time, but this effect was observed both in the normo- and hyperglycaemia treated cells (Figure 3.2A). The difference between the normo- and hyperglycaemia treated cells was most apparent 4 hours after incubation. We observed the appearance of three bands of approximately 60, 80 and 220 kDa in cells treated with 25 mM D-glucose for 4 hours. However, the bands were visible both in cells treated with 5 mM and 25 mM D-glucose when incubated for 48 and 72 hours.

Next, we examined the specificity of the immunoreactive bands using free N-acetylglucosamine (GlcNAc) as a competitor of CTD 110.6. The CTD 110.6 antibody was preincubated with 0.5 M GlcNAc for 5 minutes on ice before incubation with the western blot. Immunoreactive bands of approximately (25, 50, 60, 80, 90, 150, 250 kDa were specifically lost, indicating that the majority of the immunoreactive bands were O-GlcNAcylated proteins (Figure 3.2B).

Diabetes is characterized by chronic hyperglycaemia. Several reports studying effects of hyperglycaemia in endothelial cells incubate the cells for 48 hours or longer (85-93). To study the effects of D-glucose on protein O-GlcNAcylation levels, HUVEC treated with 1, 2.5, 5, and 25 mM D-glucose for 48 hours were lysed, and sWGA precipitation were used to enrich for N-and O-GlcNAc modified proteins. The intensity of an O-GlcNAcylated immunoreactive band of approximate 70 kDa was highest in samples treated with 1 mM compared to 2.5 mM D-glucose. Bands of approximately 100 kDa, 160 kDa and 170 kDa were nearly absent at 1 mM D-glucose, but increased from 2.5 to 25 mM D-glucose treatment (Figure 3.2C). We also observed a more distinct increase in O-GlcNAcylation from 5 to 25 mM D-glucose compared with whole cell lysates in Figure 3.2A, indicating an advantage using sWGA.

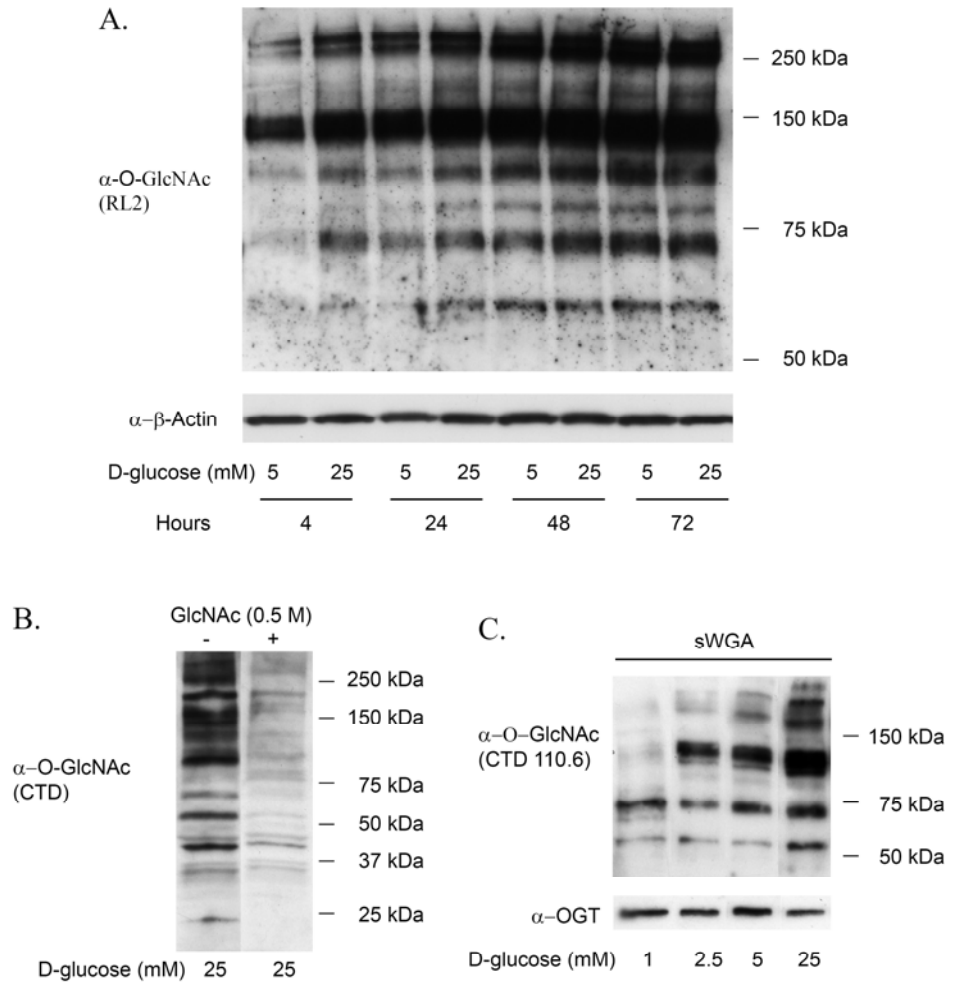

Fig. 3. 2. Time and dose effects of glucose on the level of protein O-GlcNAcylation

A. HUVEC were incubated with 5 or 25 mM D-glucose for 4, 24, 48 or 72 hours. Whole cell lysates were made and samples, (18 µg protein/lane) were analyzed by SDS-PAGE (7.5 % gel) and western blotting using the monoclonal antibody RL2 which detect a subset of O-GlcNAcylated proteins. β-Actin was used as a loading control. **B.** HUVEC were incubated with 25 mM D-glucose for 48 hours. Whole cell lysates were prepared and samples (15 µg protein/lane) analyzed by SDS-PAGE (4-20 % gel) and western blotting. 0.5 M N-acetylglucosamine (GlcNAc) (+) was used as a competitor of CTD 110.6, and O-GlcNAcylated proteins were specifically lost (+) due to the competition. **C.** HUVEC were incubated with 1, 2.5, 5 or 25 mM D-glucose for 48 hours. Whole cell lysates were prepared and the protein concentration adjusted to 0.7 µg/µl before N-and O-GlcNAcylated proteins were precipitated from 500 µl lysate using sWGA. The same amount of samples were loaded in each lane, and analyzed by SDS-PAGE (4-20 % gel) and western blotting with CTD 110.6. The antibody OGT was used as a positive control.

3.3 Effects of hyperglycaemia on LXRβ O-GlcNAcylation

It has recently been suggested that LXR is a glucose sensor in human HepG2 cells and in vivo in mouse liver (60). The direct binding of the hydrophilic glucose molecule to the hydrophobic pocket of LXR reported by Mitro et al (60) is surprising. The hydrophilic nature of the glucose molecule indicates that glucose rather may affect LXR indirectly via downstream glucose signalling pathways. LXRα/β has several potential O-GlcNAcylated sites as identified by YinOYang (1) search (Appendix A and B). For this reason we wondered whether LXR is a target for O-GlcNAc modification. HUVEC were incubated with 1, 2.5, 5 or 25 mM D-glucose for 48 hours. Whole cell lysates were made and sWGA was used to precipitate O-and N-GlcNAcylated proteins. Western blot was analyzed using the LXR antibody R20. The immunoreactive band in Figure 3.3A indicates that LXR are GlcNAcylated (Figure 3A). The antibody R20 detects both LXRα and LXRβ. In the sWGA samples we detected only one immunoreactive band of about 60 kDa (Figure 3A). In order to reveal the LXR isoform, LXRβ IP and LXRα IP were carried out. LXRα and LXRβ move differently in SDS-PAGE. The predicted size of LXRα and LXRβ immunoreactive band is approximately 50 kDa. However, we observed that LXRβ is constantly about 60 kDa in several cell types. The LXRβ IP (Figure 3.3C), revealed an immunoreactive band of the same size as the immunoreactive band observed in the sWGA samples in Figure 3.3A, indicating that the immunoreactive band in the sWGA samples represent LXRβ. LXRα IP revealed a band of 50 kDa, but the same size as the heavy chain makes it difficult to interpret (data not shown). It is reasonable to suppose that the concentration of LXRα is low in HUVEC compared with LXRβ, since it is reported that LXRα mainly is expressed in the liver, adipose tissue and macrophages, whereas LXRβ is ubiquitously expressed (54). Furthermore, preliminary data from human HepG2 cells and THP-1 cells indicate that LXRβ is target for O-GlcNAcylation.

The intensity of LXRβ in the sWGA samples (Figure 3.3A) increases with the D-glucose concentration indicating that GlcNAcylation of LXRβ increases with increasing D-glucose concentrations.

HUVEC were treated with NAG-thiazoline for 2, 6 or 24 hours to inhibit O-GlcNAcase and thereby promoting O-GlcNAc modifications. LXR is a nuclear hormone receptor, and mainly expressed in the nucleus. Nuclear extracts were prepared, O- and N-GlcNAcylated proteins were immunoprecipitated using sWGA, and samples were analyzed by western blotting. The intensity of LXRβ immunoreactive bands increased with NAG-thiazoline treatment in a time dependent manner (Figure 3.3C).

To further examine whether LXRβ is O-GlcNAcylated, we IPed LXRβ and incubated the western blot with RL2 monoclonal antibody, but did this not reveal immunoreactive bands (data not shown). We also immunoprecipitated O-GlcNAcylated proteins using RL2 antibody, but again did not observe LXRβ immunoreactive band when incubating the blot with the LXRβ specific antibody. However, Flag tagged LXRβ transfected in HepG2 was used as a positive control and the transfected LXRβ was detected by the RL2 antibody and LXRβ, indicating that LXRβ is a target for O-GlcNAcylation (data not shown).

To study whether LXRβ protein level is regulated by different D-glucose concentrations in HUVEC, cells were incubated with 1 mM, 2.5 mM, 5 mM or 25 mM for 48 hours. Whole cell lysates were analyzed by SDS-PAGE and western blotting. Figure 3.3A shows that LXRβ protein level is not regulated by different D-glucose concentrations when incubated for 48 hours.

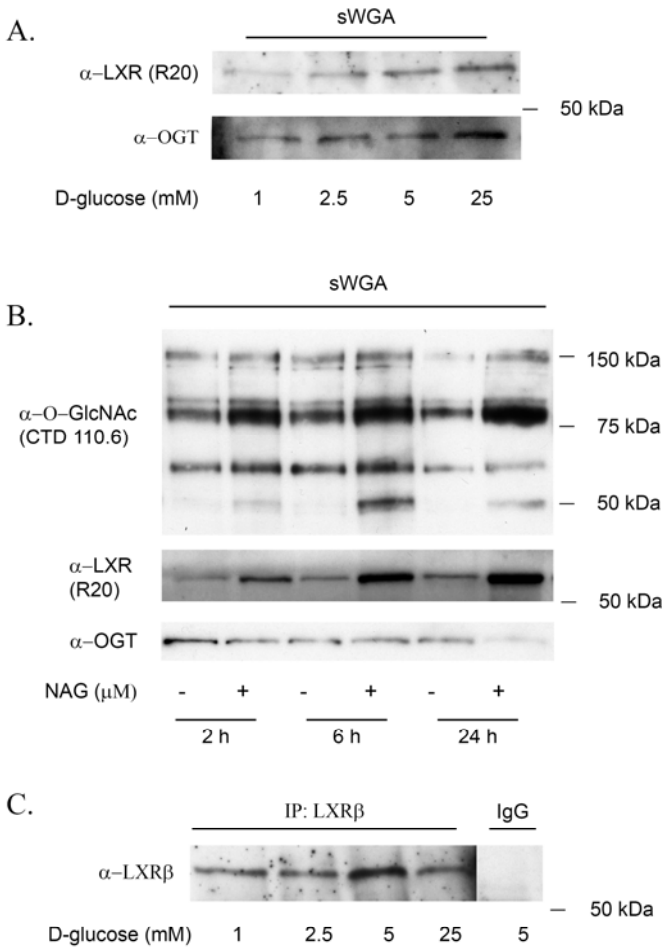

Fig. 3.3. Effects of glucose on O-GlcNAcylation of LXR

A. HUVEC were treated with 1, 2.5, 5 or 25 mM D-glucose for 48 hours. Whole cell lysates were prepared and the protein concentration adjusted to 0.7 µg/µl before N-and O-GlcNAcylated proteins were precipitated from 500 µl lysate using sWGA. The same amount of samples were loaded in each lane, and analyzed by SDS-PAGE (4-20 % gel) and western blotting using the antibody R20 detecting LXRα/β. OGT was included as a positive control. **B.** HUVEC were incubated with 10 µM NAG and harvested 2, 6 and 24 hours after incubation. Nuclear extracts were made, and the protein concentrations were adjusted to 0.9 µg/µl, before N-and O-GlcNAcylated proteins were precipitated from 500 µl lysate using sWGA. The same amount of samples were loaded in each lane and analyzed by SDS-PAGE and western blotting using a specific antibody against LXRβ. The antibody OGT was included as a positive control. **C.** HUVEC were treated with 1, 2.5, 5 or 25 mM D-glucose for 48 hours. Whole cell lysates were prepared and the protein concentration adjusted to 0.7 µg/µl. LXRβ was immunoprecipitated from 500 µl lysate and the same amount of samples were loaded into each lane and analyzed by SDS-PAGE and western blotting using a specific antibody against LXRβ.

3.4 Effects of glucose on Id1 and Id3 protein expression and O-GlcNAcylation

D-glucose is reported to affect the expression of Id proteins, but the response differ according to cell type (65;70). Whether D-glucose induces the expression of Id proteins in HUVEC have not previously been examined. In our experiments, Id2 was not detected in HUVEC and glucose failed to induce the Id2 protein expression (data not shown). In the following experiments we thus focused on Id1 and Id3 proteins.

Preliminary experiments in the present study indicated that hyperglycaemia for 4-24 hours did not regulate the expression of Id1 and Id3 proteins (data not shown).

It is reported that agents (eg. D-glucose, TSH) induce a biphasic pattern of Id expression (70;94), and it is suggested that Id proteins could regulate rapid as well as long term responses to changes in glucose concentrations.

To study the effects of chronic D-glucose exposure on Id1 and Id3 protein expression in HUVEC, cells were treated with 1, 2.5, 5 or 25 mM D-glucose for 48 hours. The Id1 immunoreactive bands observed did not differ in intensity, indicating that Id1 protein levels were not affected by different D-glucose concentrations at this time point (Figure 3.4A). In contrast, the Id3 protein levels increased with increasing D-glucose concentrations (Figure 3.4A).

We incubated cells with different NAG-thiazoline concentrations for 24 hours in order to promote O-GlcNAcylation. Prolonged treatment with the O-GlcNAcase inhibitor PUGNAc is not toxic to cells, but treatment above 18 hours do not result in additional increase in O-GlcNAcylation (48). Whole cell lysates were analyzed by SDS-PAGE and western blotting using Id1 and Id3 specific antibodies. The Id1 protein levels were not affected by NAG-thiazoline treatment as indicated by the same intensity of the immunoreactive bands (Figure 3.4B). However, the expression of Id3 protein increased with increasing NAG-thiazoline concentrations (Figure 3.4B).

YinOYang (1) search for potential Id O-GlcNAcylation sites suggests that Id1 has 5 potential O-GlcNAc sites, including one high score site at serine 16 and one site at serine 130 predicted to be target for both phosphorylation and O-GlcNAcylation (Appendix C). In contrast, Id3 has only one low score potential O-GlcNAc site at serine 116 (Appendix D).

In order to study whether Id1 protein are O-GlcNAcylated, HUVEC were incubated with 1, 2.5 , 5 or 25 mM D-glucose for 48 hours, whole cell lysates were prepared and Id1 was immunoprecipitated. The samples were analyzed by immunoblotting using the monoclonal antibody CTD 110.6. We detected bands of approximately 15 and 20 kDa (Figure 3.4C). The bands differed in intensity with the strongest intensity at 2.5 mM D-glucose and the weakest intensity at 25 mM D-glucose. The blots were stripped and reprobed with a polyclonal antibody against Id1, revealing bands of the same size (Figure 3.4C).

The level of immunoprecipitated Id1 differed between the samples (Figure 4C), with the highest level at 2.5 mM D-glucose and the lowest level at 25 mM D-glucose coinciding with the Id1 O-GlcNAc levels. This phenomenon was seen in different experiments and time points.

RL2 monoclonal antibody was used to immunoprecipitate O-GlcNAcylated proteins. Cells treated with 5 and 25 mM D-glucose for 48 hours was lysed, and RL2 immunoprecipitated proteins were analyzed by immunoblotting. Immunoblot of RL2-IP samples with a polyclonal Id1 antibody revealed an immunoreactive band of approximately 15 kDa, suggesting that Id1 is O-GlcNAcylated (Figure 3.4D). The total Id1 protein levels increased from 5 mM D-glucose to 25 mM D-glucose, indicating that hyperglycaemic conditions increase the level of O-GlcNAc modifications on Id1 protein. The blot was reprobed with RL2 antibody and Figure 3.4D show an increase in the level of O-GlcNAcylated proteins when exposed to hyperglycaemia.

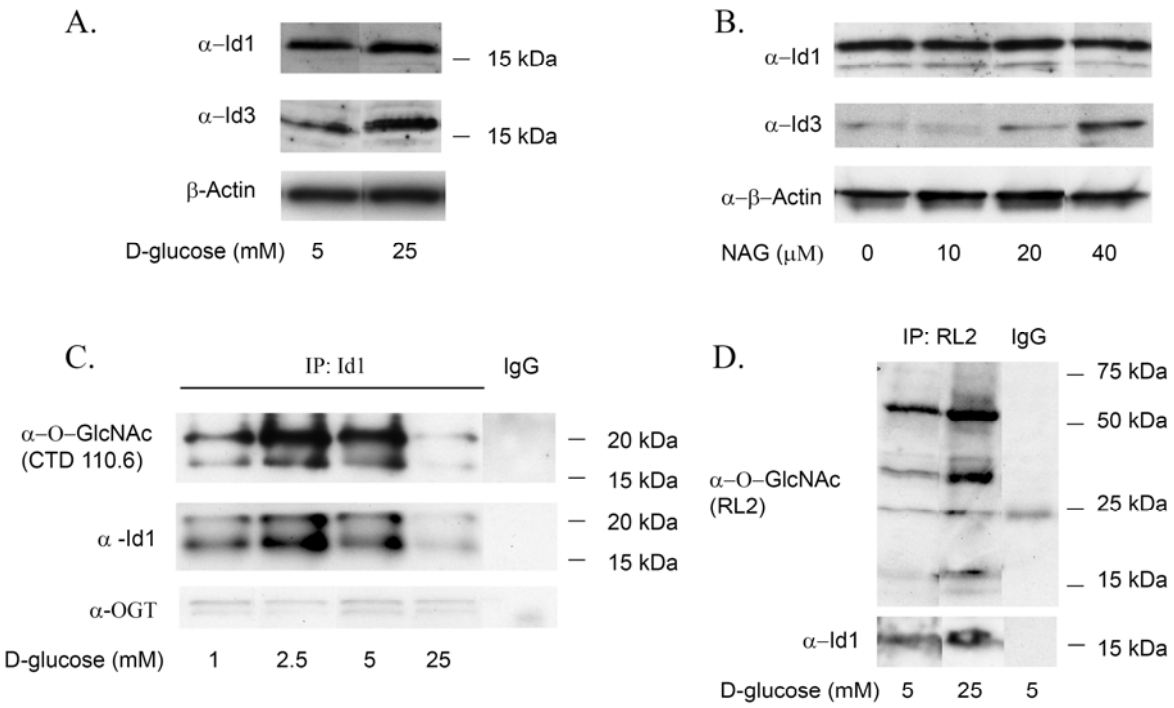

Fig. 3.4. Effects of glucose on Id1 and Id3 protein expression and O-GlcNAcylation

A. HUVEC were incubated with 5 or 25 mM D-glucose for 48 hours and **B.** 0, 10, 20 and 40 μM NAG for 24 hours. Whole cell lysates were prepared and 22.5 μg protein were loaded into each lane, separated by SDS-PAGE (4.20 % gel) and analyzed by immunoblotting using polyclonal antibodies against Id1 and Id3 proteins. β-Actin was used as a loading control. **C.** HUVEC were incubated with 1, 2.5, 5 or 25 mM D-glucose for 48 hours, whole cell lysates were prepared and the protein concentrations adjusted to 1.1 μg/μl. Id1 proteins were immunoprecipitated from 500 μl lysate. The same amount of samples were loaded into each lane and analyzed by immunoblotting (4-20 % gel) using the monoclonal antibody CTD 110.6 against O-GlcNAcylated proteins. The membrane was stripped and reprobed with a polyclonal antibody against Id1. **D.** HUVEC were incubated with 5 mM or 25 mM D-glucose for 48 hours, whole cell lysates were prepared and the protein concentrations adjusted to 0.7 μg/μl. O-GlcNAcylated proteins were immunoprecipitated from 500 μl lysate using the RL2 antibody. The samples were analyzed by SDS-Page (4-20 % gel) and western blotting using Id1 polyclonal antibody. The membrane was stripped and reprobed with the monoclonal antibody RL2 and a light chain specific secondary antibody.

4. Discussion

4.1 Concentration and time dependent effects of NAG-thiazoline on O-GlcNAcylation

PUGNAc and NAG-thiazoline are used to inhibit O-GlcNAcase, thus promoting O-GlcNAc modification on intracellular proteins. NAG-thiazoline is not commercially available, and the optimal concentration in HUVEC is not known, but it is reported to be more potent than PUGNAc (49).

We found that 10 μM NAG-thiazoline is sufficient to promote O-GlcNAcylation in HUVEC. This is 10 fold less than the optimal dose of PUGNAc used to promote O-GlcNAc modification in several different cell types (46;81-84). In adipocytes incubated with varying concentrations of PUGNAc for 12 hours, the maximal increase in O-GlcNAc levels appeared at 100 μM PUGNAc, and no further increase in O-GlcNAc level was seen in cells treated with higher concentrations (95).

O-GlcNAcylation is a dynamic process. We investigated O-GlcNAc levels in HUVEC treated with 10 μM NAG-thiazoline at different time points. The level of O-GlcNAc modifications increased significantly with time. This is comparable with other studies using PUGNAc. Adipocytes incubated with 100 μM PUGNAc displayed a modest increase in O-GlcNAc levels in cells treated for 6 hours, whereas cells treated for 12 hours showed a considerable increase in O-GlcNAc levels (95).

A single protein may show different optimal time for maximal O-GlcNAcylation as compared to overall O-GlcNAcylation level. PUGNAc treatment in SH-SY5Y neuroblastoma cells caused an overall increase in O-GlcNAcylation level after 60 minutes of treatment, whereas maximal O-GlcNAc modification of Akt1 occurred 30 minutes after treatment (96). In sWGA samples in Figure 1B, OGT was used as a positive control. The maximal O-GlcNAcylation of OGT appeared 2 hours after

NAG-thiazoline treatment, whereas the maximal overall O-GlcNAcylation appeared 24 hours after treatment.

4.2 Effects of glucose on the level of protein O-GlcNAcylation in HUVEC

Hyperglycaemia is associated with endothelial dysfunction and increased risk of micro- and macrovascular complications. Increased levels of protein O-GlcNAcylation may be a molecular mechanism by which hyperglycaemia induce endothelial dysfunction and thus contribute to the pathogenesis of vascular complications.

Hyperglycaemia is shown to increase the total level of O-GlcNAcylated proteins in different cell types; Rin-m5f cells (rat pancreatic β-cell line), HepG2 cells and rat smooth muscle cells (72;97;98). One specific aim of this study was to elucidate whether hyperglycaemia (25 mM) increases the level of O-GlcNAcylated proteins in HUVEC, and we found in agreement with other reports that hyperglycaemia increases the level of O-GlcNAcylated proteins in a time dependent manner. However, we also observed increases in levels of O-GlcNAc modified proteins in normoglycaemic (5 mM) treated cells (Figure 3.2A), indicating time-in-culture effects.

In the literature, we have observed that the normoglycaemia (5 mM) control samples for each time point seldom are presented (81;96;97;99). We have not found reports presenting total protein O-GlcNAcylation levels of glucose treatment for more than 24 hours with normoglycaemia control samples. Taylor et al found no increase in total O-GlcNAcylation in HepG2 cells treated with 5 mM D-glucose for 1- 24 hours (98).

Before incubation with different D-glucose concentrations, the MCDB medium containing 5 mM D-glucose was changed to RPMI 1640 medium added the same concentration of D-glucose and FBS (7 %), but lacking the growth factors and

antibiotics. The next morning, the cells were incubated with RPMI 1640 containing different concentrations of D-glucose. The medium was replaced every 24 hours in order to maintain the D-glucose concentration and to avoid any secondary autocrine effects of glucose. We do not know the reason for the increase in O-GlcNAcylation in the 5 mM control samples with time in culture. All cells were treated identically, except from incubation with different D-glucose concentrations. We can not, however, exclude the possibility that other factors than glucose may have induced the increase in O-GlcNAcylation seen with time.

HUVEC is sensible to serum starvation, especially when lasting for more than 24 hours (100). For longer experiments, the absence of growth factors triggers apoptosis. In our experiments, we used 7 % FBS. FBS is a complex mixture containing, besides growth factors, a variety of proteins, lipids, glucose, salts, minerals, amino acids, growth hormones, trace elements and other factors not fully identified (http:/www.sigmaaldrich.com). The hexosamine signalling pathway is a nutrient signalling pathway (28;29;101) and it is possible that constituents in the FBS may have affected the level of O-GlcNAcylation. The boost of FBS each 24 hour may have triggered O-GlcNAcylation with time, possibly via activation or increased level of GFAT or OGT.

In order to examine whether the immunoreactive bands induced by hyperglycaemia were specific, HUVEC were subject for competition experiments with free GlcNAc. The majority of the immunoreactive bands (25, 50, 60, 80, 90, 150, 250 kDa) were specifically lost due to the competition. The sizes of the immunoreactive bands are comparable with the NAG-thiazoline induced immunoreactive bands in Figure 1.

A number of studies have reported that acute activation of O-GlcNAc formation is a cytoprotective stress response. However, sustained increases in O-GlcNAc have been associated with the pathogenesis of diabetes and diabetic complications (102).

When studying effects of hyperglycaemia in endothelial cells, the literature indicates distinct effects when cells are treated with hyperglycaemia for 48 hours and above. It

is shown that hyperglycaemia induced marked increase in O-GlcNAcylation of IRS-1, IRS-2 and p85, resulting in insulin resistance in human coronary artery endothelial cells (HCAEC) incubated for 72 hours (52). Du et al (87) showed that hyperglycaemia for 48 hours in BAEC increased O-GlcNAcylation of SP1.

To study the effects of different glucose concentrations on the level of O-GlcNAcylated proteins, HUVEC were incubated with 1, 2.5, 5 or 25 mM D-glucose in RPMI 1640 medium for 48 hours. Succynilated WGA was used to enrich the lysates of GlcNAcylated proteins. Figure 3.2C show that increased concentration of D-glucose induced an increased level of O-GlcNAcylation. The difference in O-GlcNAcylation between normo- (5 mM) and hyperglycaemia (25 mM) treated cells (Figure 3.2C) were more distinct than the increase observed between the 48 hour treated normo- and hyperglycaemia treated cells in Figure 3.2A, indicating an advantages to use sWGA.

In the same experiment (Figure 3.2C), we observed that a 70 kDa immunoreactive band displayed increased intensity in both hypo- and hyperglycaemia treated cells. An immunoreactive band of approximately 100 kDa and two high molecular bands were nearly absent in the samples from cell treated with 1 mM D-glucose (Figure 3.2C). Hypoglycaemia is a stressful situation, and stress is known to induce O-GlcNAc modifications and promote cell survival. In glucose sensitive cells (liver cells and neuroblastoma cells), glucose deprivation induced a significant increase in the level of O-GlcNAcylated proteins 6-24 hours after deprivation (98;99).

Several of the O-GlcNAc targets induced were distinct from those modified in response to hyperglycaemia. Cells incubated with 1 mM D-glucose did however, not show a marked stress induced increase in O-GlcNAcylation. We did not observe induction of unique immunoreactive bands or increased level of O-GlcNAcylation, indicating that the effect was not a general stress response. It is not, however, unlikely that individual proteins may show different sensitivities to stress. The level of confluence is also observed to influence the effect of glucose deprivation. Taylor et al observed that 70 % confluence was optimal for promoting glucose deprivation in

HepG2 cells. Under- and over- confluent cells displayed a reduced effect (98). In our experiments, the cells were 80-100 % confluent as observed in the microscope.

It has been suggested that hyperglycaemic peaks may play a significant role in the pathogenesis of vascular diabetic complications (15;103). Levels of postprandial plasma glucose appear to be a stronger predictor of cardiovascular disease than stable elevated plasma glucose (104). Intermittent treatment with hyperglycaemia (24 hour cycles) for 7-14 days is shown to induce a greater increase in the levels of the adhesion molecules ICAM-1, VCAM-1 and E-selectin than stable hyperglycaemia (105). For future studies, intermittent glucose load on the level of O-GlcNAcylated proteins will be an interesting subject for examination.

One future aim is to identify glucose or NAG-thiazoline induced O-GlcNAcylated proteins by mass spectrometry. PNGase F treatment (96) will remove all N-linked GlcNAcylations and O-GlcNAcylated proteins are immunoprecipitated using sWGA. Immunoactive bands on western blot will than be analyzed by mass spectrometry.

4.3 Effects of glucose on LXR O-GlcNAcylation

LXR are nuclear receptors that coordinate carbohydrate and lipid metabolism. Oxysterols are known LXR ligands, but recently it was reported that LXR activity was regulated by direct binding of D-glucose (60) and D-glucose was able to induce the expression of the LXR target gene ABCA1 (60).

ABCA1 promotes the efflux of free cholesterol and phospholipids from cells to lipid-poor apolipoproteins A-1 (apoA-1) to generate nascent High density lipoproteins (HDL)-particles. LXR function in endothelial cells has not been extensively studied. It is reported that ABCA1 is a LXR target gene in HUVEC involved in reverse cholesterol transport to Apo-A1 in the vascular lumen. ABCA1 in HUVEC is up-regulated by LDL (55) and down-regulated by oxLDL (56). Endothelial cells express oxLDL receptors. Since endothelial cells rarely accumulate lipids, it was hypothesized that oxLDL-induced down-regulation of ABCA1 leads to efflux of

cholesterol to the subendothelial space via caveolae. The changed transport route may lead to subendothelial deposition of lipids and plaque formation in the intima (56).

The direct binding of the hydrophilic glucose molecule to the hydrophobic pocket of LXR reported by Mitro et al (60) is surprising. The hydrophilic nature of the glucose molecule indicates that glucose rather may affect LXR indirectly via downstream glucose signalling pathways. Earlier studies have shown that LXR are posttranslationally modified by phosphorylation (106), acetylation (107) and sumoylation (108).

Both, LXRα and -β have several potential O-GlcNAcylation sites (Appendix A and B), and O-GlcNAcylation may be a mechanism by which LXR is posttranslationally modified and affected by glucose. The predicted size of LXRα and LXRβ immunoreactive band is approximately 50 kDa. However, we observed that LXRβ is constantly about 60 kDa in several cell types. LXRβ IP in HUVEC revealed an immunoreactive band of about 60 kDa, indicating that the immunoreactive band of about 60 kDa detected by the antibody R20 in the sWGA samples is LXRβ. LXRα immunoreactive bands of 50 kDa were not detected by the R20 antibody in the sWGA samples. This is probably due to low concentration of LXRα in HUVEC.

To further study whether LXRβ is O-GlcNAcylated, LXRβ was immunoprecipitated from whole cell extracts and analyzed by western blotting using the antibodies RL2 or CTD 110.6. However, LXRβ was not detected. The samples were resuspended in 80 µl loading dye in order to be able to analyze parallel gels, leading to lower LXR concentration, and this may be one possible explanation for the negative results. Flag tagged LXRβ transfected in HepG2 cells was used as a positive control, and transfected flag tagged LXRβ from HepG2 cells was detected by the RL2 antibody (data not shown). This indicates that LXRβ is a potential target for O-GlcNAcylation. The difference seen may be due to different cell types or higher protein concentration in the transfected cells.

To further study whether LXRβ is a target for O-GlcNAcylated in HUVEC, it may be necessary to overexpress LXR in order to increase the protein concentration and to analyze the whole IP on one gel. Immunoprecipitation from nuclear lysates or upscaling the IP may further increase the concentration. To confirm the results and identify O-GlcNAcylation site, mass spectrometric analysis will be performed.

4.4 Effects of glucose on Id1 and Id3 protein expression and O-GlcNAcylation

D-glucose is reported to affect the expression of Id proteins, but the response differ according to cell type (65;70). Hyperglycaemia is shown to induce Id1 mRNA and Id1 protein in pancreatic β-cells. Hyperglycaemia also induce the level of Id1 mRNA in CaCo-2 cells, but has no effect on the level of Id1 and Id3 mRNA in BC3H1 or HepG2 cells (70). In murine J774.2 macrophages hyperglycaemia induce an increased level of Id2 protein (75).

Effects of glucose on Id proteins in HUVEC have not previously been studied. Our data indicates that Id3 is, in contrast to Id1, regulated by different D-glucose concentrations when incubated for 48 hours. Even though it has been demonstrated that Id1 and Id3 have similar promoter sequence and the pattern of Id1 expression most closely resembles that of Id3, it is reported that they are regulated differently by Fluvastatin (109), a 3-hydroxyl-3-methylglutaryl-coenzyme A (HMG-CoA) reductase inhibitor. Statins is used to lower cholesterol levels in patients (110), and it can also regulate angiogenesis (109).

HUVEC can survive in serum-free medium for up to 12 hours without losing their phenotypic features. For longer experiments, in particular those lasting more than 24 hours, the absence of growth factors triggers apoptosis (100). We replaced the endothelial basal medium (MCDB131) with RPMI1640 medium during experiments. When the cells were grown in RPMI with low serum, they appeared to grow somewhat differently than when the serum was maintained at the same level as

during culturing. We thus kept the FBS concentration at 7 % also during experiments, and this may have confounded the results. Serum is shown to induce Id1 and Id2 mRNA (61;111), and Id3 was first identified as a serum-inducible gene (65). Preliminary data performed in this study indicates that Id1 protein may be regulated by glucose when grown in 2 % serum. The experiment is however performed only once, so conclusions can not yet be drawn.

Glucose has been shown to induce a biphasic increase in Id1 and Id3 mRNA and Id1 protein, with highest expression 30 minutes after addition of D-glucose. Thereafter, the concentration decreased for 2 hours, before steadily increasing for 24 hours (70). Based on the biphasic time pattern, it is suggested that Id proteins could regulate rapid as well as long term responses to changes in D-glucose concentrations. We incubated the cells with D-glucose for 48 hours, focusing on chronic hyperglycaemia. We found that Id1 protein did not seem to be regulated by chronic hyperglycaemia in HUVEC, but we can not, however, rule out that Id1 may be regulated by acute (15 minutes-4 hours) hyperglycaemia. It is also not known whether intermittent hyperglycaemia affects Id proteins. Fasting and refeeding is reported to regulate Id expression in rainbow trout (112), and it would be interesting to study the effects of intermittent hyperglycaemia on the level of Id proteins in human endothelial cells.

Our data indicates that Id3 protein levels are up-regulated by increasing NAG-thiazoline concentrations, indicating that O-GlcNAcylation may regulate Id3 protein expression. Several transcription factors are known to be O-GlcNAcylated (113). Hyperglycaemia is shown to induce O-GlcNAcylation of the ubiquitous transcription factor Sp1 (84;87). Sp1 is shown to regulate Id1 (114) and Id4 (115). In order to further elucidate whether Id3 is regulated via the hexosamine signalling pathway, more studies are needed. GFAT requires glutamine for normal function, and incubating cells with medium lacking glutamine, incubate cells with the GFAT inhibitor DON, or incubate cells with glucosamine which is acting downstream of GFAT, may establish our findings.

Preliminary experiments in our group indicate that Id2 is target for O-GlcNAcylation (76). To study whether Id1 is target of O-GlcNAcylation in HUVEC, cells were incubated with different D-glucose concentrations, whole cell lysates were prepared, Id1 or O-GlcNAcylated protein were immunoprecipitated, and the samples analyzed by immunoblotting. A 15 kDa CTD110.6 immunoreactive band was detected in Id1 immunoprecipitates and Id1 was detected in RL2 immunoprecipitates, indicating that Id1 is target for O-GlcNAcylation. We are, however, not able to conclude whether D-glucose up-regulates O-GlcNAcylation of Id1, because the level of immunoprecipitated proteins differed between the samples. The IPs were carried out from lysates containing the same amount of proteins. We do not know why the level of immunoprecipitated proteins differed between the samples. The Id1 polyclonal antibody is raised against a peptide mapping to the C-terminus of Id protein. Id1 has two potential O-GlcNAc sites in the C-terminus, and we speculate that O-GlcNAcylation of Id1 may interfere with the binding of the antibody to Id1.

Formation of new blood vessels into an atherosclerotic plaque is associated with increased risk of fatal outcome. The immature vessels leak erythrocytes (cholesterol rich membranes) and inflammatory cells into the core of the plaque. Several new vessels increase the risk of intra plaque haemorrhages and rupture (116;117). Intra plaque haemorrhage is shown to be increased in plaques from diabetic patients (71). Activated T-cells, macrophages and mast cells in the atherosclerotic plaque produce proangiogenic molecules such as VEGF and IL8 (116). VEGF is shown to induce the expression of Id1 and Id3 in HUVEC (74). There are similarities between vessels of tumours and plaque vessels. Both, tumours and plaques require oxygen and thus new blood vessels when the size limits the diffusion of oxygen (116). Id proteins are thought to facilitate angiogenesis in tumours (67;69). It is shown that overexpression of Id can induce proliferation, activation (increased the expression of ICAM-1 and E-selectin) and angiogenic processes in HUVEC (transmigration, expression of matrix metalloproteinases-2 and –9, and tube formation) (74). The effects of hyperglycaemia on angiogenesis are not fully understood (72). Both, up- and down regulation of angiogenesis in different tissues have been reported as a consequence of

hyperglycaemia. It would be interesting to study whether hexosamine induced up-regulation of Id3 or O-GlcNAcylation of Id1 may affect angiogenic processes in HUVEC.

4.5 HUVEC

Primary cells are more heterogeneous than cell lines. The differences we found in some of the experiments may reflect variations in lifestyle and genetic constituents between the individual HUVEC donors. The cells were grown under the same culture conditions for up to 3 weeks prior to each experiment, and this will probably reduce potential differences.

Blood vessels and the function of the endothelial cells vary according to location (5;118). The expression of GFAT is for example shown to vary between small and medium sized vessels of various organs (35), indicating differences in O-GlcNAcylation between different vascular beds).

Specific arterial and venous gene expression pattern have been identified (118). HUVEC are endothelial cells from a vein transporting arterial blood from the placenta to the foetus. Endothelial cells isolated from umbilical cords are readily available and a valuable source to study glucose induced endothelial dysfunction, but one should bear in mind that their properties may differ from other types of endothelial cells (21;80;100;118).

To my knowledge, O-GlcNAcylation has not been studied in HUVEC. One advantage using HUVEC is that our lab has access to human umbilical cords and has long expertise in isolating HUVEC. Increasing evidence show however, that endothelial cells isolated from HUVEC differ in their responses to agonists in comparison to arterial endothelial cells (119). HUVEC thus has its limitations as a model system when studying glucose induced endothelial dysfunction as an early event in atherosclerosis. Experiments in HUVEC should be followed by experiments

in the less available and more expensive human artery endothelial cells (HAEC) or human coronary artery endothelial cells (HCAEC).

5. Conclusions

The results of this study indicate that:

- The O-GlcNAcase inhibitor NAG-thiazoline is 10 times more potent than PUGNAc on protein O-GlcNAcylation in HUVEC, and 10 μM is sufficient to induce an increase in overall O-GlcNAcylation in HUVEC.

- Hyperglycaemia increases protein O-GlcNAcylation in HUVEC in a time dependent manner. However, because we also observed an increase in O-GlcNAcylation in the normoglycaemia treated control samples with time, firm conclusions can not yet be drawn. It is necessary to optimalise the culturing conditions during experiments, allowing for serum free conditions. Succinylated WGA to precipitate GlcNAcylated proteins prior to SDS-PAGE and western blot analysis reveal a more distinct difference in total O-GlcNAcylation between cells cultured in normo- versus high glycaemic conditions.

- Id1 protein is a target for O-GlcNAcylation and Id1 expression is not regulated by chronic D-glucose exposure in HUVEC. This is in contrast to Id3. However, the FBS concentration used during experiments may have confounded the observed results and further studies are needed in order to make firm conclusions.

- LXRβ is a promising candidate for O-GlcNAcylation. Our data indicates that LXRβ is target for GlcNAcylation as indicated by sWGA precipitation experiments, but more studies are needed in order to conclude whether LXRβ is a target for GlcNAcylation and to identify the nature of the GlcNacylation.

6. Reference list

1. YinOYang 1.2 Prediction server. http://www.cbs.dtu.dk/services/YinOYang/. 2008.
2. Shils ME, Shike M, Ross AC, Caballero B, Cousins RJ. Modern Nutrition in health and disease. Lippincott Williams & Wilkins, 2006.
3. Champe PC HR. Lippincott`s Illustrated Reviews: Biochemistry. J.B. Lippincott Company, 1994.
4. Schwartz MW, Woods SC, Porte D, Jr., Seeley RJ, Baskin DG. Central nervous system control of food intake. Nature 2000;404:661-71.
5. Cersosimo E, DeFronzo RA. Insulin resistance and endothelial dysfunction: the road map to cardiovascular diseases. Diabetes Metab Res Rev 2006;22:423-36.
6. Kopelman PG. Obesity as a medical problem. Nature 2000;404:635-43.
7. Ludwig DS. The glycemic index: physiological mechanisms relating to obesity, diabetes, and cardiovascular disease. JAMA 2002;287:2414-23.
8. WHO. Fact sheet no 312. Diabetes. 2006.
9. WHO. Definition and diagnosis of diabetes mellitus and intermediate hyperglycemia. 2006. Ref Type: Report
10. Schalkwijk CG, Stehouwer CD. Vascular complications in diabetes mellitus: the role of endothelial dysfunction. Clin Sci (Lond) 2005;109:143-59.
11. Sosial- og helsedirektoratet. Utviklingen i norsk kosthold 2007. 2007. Ref Type: Report
12. Nordic Council of Ministers. Nordic Nutrition Recommendations 2004. Norden, 2004.
13. Thomas B. Manual of Dietetic Practice. Blackwell Publishing Company, 2001.
14. Frayn KN. Metabolic Regulation. A human Perspective. Blackwell Publishing, 2003.
15. O'Keefe JH, Bell DS. Postprandial hyperglycemia/hyperlipidemia (postprandial dysmetabolism) is a cardiovascular risk factor. Am J Cardiol 2007;100:899-904.
16. Shimabukuro M, Chinen I, Higa N, Takasu N, Yamakawa K, Ueda S. Effects of dietary composition on postprandial endothelial function and adiponectin concentrations in healthy humans: a crossover controlled study. Am J Clin Nutr 2007;86:923-8.
17. Bianchi C, Miccoli R, Penno G, Del PS. Primary prevention of cardiovascular disease in people with dysglycemia. Diabetes Care 2008;31 Suppl 2:S208-S214.
18. Giugliano D, Ceriello A, Esposito K. Glucose metabolism and hyperglycemia. Am J Clin Nutr 2008;87:217S-22S.

19. Brownlee M. Biochemistry and molecular cell biology of diabetic complications. Nature 2001;414:813-20.

20. Brownlee M. The pathobiology of diabetic complications: a unifying mechanism. Diabetes 2005;54:1615-25.

21. Nachman RL, Jaffe EA. Endothelial cell culture: beginnings of modern vascular biology. J Clin Invest 2004;114:1037-40.

22. Creager MA, Luscher TF, Cosentino F, Beckman JA. Diabetes and vascular disease: pathophysiology, clinical consequences, and medical therapy: Part I. Circulation 2003;108:1527-32.

23. Reusch JE, Draznin BB. Atherosclerosis in diabetes and insulin resistance. Diabetes Obes Metab 2007;9:455-63.

24. Libby P. Inflammation in atherosclerosis. Nature 2002;420:868-74.

25. Corti R, Hutter R, Badimon JJ, Fuster V. Evolving concepts in the triad of atherosclerosis, inflammation and thrombosis. J Thromb Thrombolysis 2004;17:35-44.

26. Wild S, Roglic G, Green A, Sicree R, King H. Global prevalence of diabetes: estimates for the year 2000 and projections for 2030. Diabetes Care 2004;27:1047-53.

27. WHO. http://www.who.int/features/factfiles/diabetes/01_en.html. 2008.
Ref Type: Slide

28. Obici S, Rossetti L. Minireview: nutrient sensing and the regulation of insulin action and energy balance. Endocrinology 2003;144:5172-8.

29. Love DC, Hanover JA. The hexosamine signaling pathway: deciphering the "O-GlcNAc code". Sci STKE 2005;2005:re13.

30. Marshall S. Role of insulin, adipocyte hormones, and nutrient-sensing pathways in regulating fuel metabolism and energy homeostasis: a nutritional perspective of diabetes, obesity, and cancer. Sci STKE 2006;2006:re7.

31. Hart GW, Housley MP, Slawson C. Cycling of O-linked beta-N-acetylglucosamine on nucleocytoplasmic proteins. Nature 2007;446:1017-22.

32. Fulop N, Marchase RB, Chatham JC. Role of protein O-linked N-acetyl-glucosamine in mediating cell function and survival in the cardiovascular system. Cardiovasc Res 2007;73:288-97.

33. Wells L, Hart GW. O-GlcNAc turns twenty: functional implications for post-translational modification of nuclear and cytosolic proteins with a sugar. FEBS Lett 2003;546:154-8.

34. Paterson AJ, Kudlow JE. Regulation of glutamine:fructose-6-phosphate amidotransferase gene transcription by epidermal growth factor and glucose. Endocrinology 1995;136:2809-16.

35. Nerlich AG, Sauer U, Kolm-Litty V, Wagner E, Koch M, Schleicher ED. Expression of glutamine:fructose-6-phosphate amidotransferase in human tissues: evidence for high variability and distinct regulation in diabetes. Diabetes 1998;47:170-8.

36. Hu Y, Riesland L, Paterson AJ, Kudlow JE. Phosphorylation of mouse glutamine-fructose-6-phosphate amidotransferase 2 (GFAT2) by cAMP-dependent protein kinase increases the enzyme activity. J Biol Chem 2004;279:29988-93.

37. DeHaven JE, Robinson KA, Nelson BA, Buse MG. A novel variant of glutamine: fructose-6-phosphate amidotransferase-1 (GFAT1) mRNA is selectively expressed in striated muscle. Diabetes 2001;50:2419-24.

38. Traxinger RR, Marshall S. Coordinated regulation of glutamine:fructose-6-phosphate amidotransferase activity by insulin, glucose, and glutamine. Role of hexosamine biosynthesis in enzyme regulation. J Biol Chem 1991;266:10148-54.

39. Weigert C, Klopfer K, Kausch C et al. Palmitate-induced activation of the hexosamine pathway in human myotubes: increased expression of glutamine:fructose-6-phosphate aminotransferase. Diabetes 2003;52:650-6.

40. Marshall S, Bacote V, Traxinger RR. Discovery of a metabolic pathway mediating glucose-induced desensitization of the glucose transport system. Role of hexosamine biosynthesis in the induction of insulin resistance. J Biol Chem 1991;266:4706-12.

41. Slawson C, Housley MP, Hart GW. O-GlcNAc cycling: how a single sugar post-translational modification is changing the way we think about signaling networks. J Cell Biochem 2006;97:71-83.

42. Zachara NE. The sweet nature of cardioprotection. Am J Physiol Heart Circ Physiol 2007;293:H1324-H1326.

43. Whelan SA, Hart GW. Proteomic approaches to analyze the dynamic relationships between nucleocytoplasmic protein glycosylation and phosphorylation. Circ Res 2003;93:1047-58.

44. Zachara NE, Hart GW. Cell signaling, the essential role of O-GlcNAc! Biochim Biophys Acta 2006;1761:599-617.

45. Lazarus BD, Roos MD, Hanover JA. Mutational analysis of the catalytic domain of O-linked N-acetylglucosaminyl transferase. J Biol Chem 2005;280:35537-44.

46. Yang X, Ongusaha PP, Miles PD et al. Phosphoinositide signalling links O-GlcNAc transferase to insulin resistance. Nature 2008;451:964-9.

47. Gao Y, Wells L, Comer FI, Parker GJ, Hart GW. Dynamic O-glycosylation of nuclear and cytosolic proteins: cloning and characterization of a neutral, cytosolic beta-N-acetylglucosaminidase from human brain. J Biol Chem 2001;276:9838-45.

48. Zachara NE, Hart GW, Cole RN, Gao Y. Detection and analysis of proteins modified by O-linked N-acetylglucosamine. Curr Protoc Mol Biol 2002;Chapter 17:Unit.

49. Knapp S, Vocadlo D, Gao Z, Kirk B, Lou J, Withers SG. NAG-thiazoline, An N-Acetyl-β-hexosaminidase Inhibitor That Implicates Acetamido Participation. J Am Chem Soc 1996;118:6804-5.

50. Akimoto Y, Hart GW, Hirano H, Kawakami H. O-GlcNAc modification of nucleocytoplasmic proteins and diabetes. Med Mol Morphol 2005;38:84-91.

51. Chatham JC, Not LG, Fulop N, Marchase RB. HEXOSAMINE BIOSYNTHESIS AND PROTEIN O-GLYCOSYLATION: THE FIRST LINE OF DEFENSE AGAINST STRESS, ISCHEMIA, AND TRAUMA. Shock 2007.

52. Federici M, Menghini R, Mauriello A et al. Insulin-dependent activation of endothelial nitric oxide synthase is impaired by O-linked glycosylation modification of signaling proteins in human coronary endothelial cells. Circulation 2002;106:466-72.

53. Maiti R, Agrawal NK. Atherosclerosis in diabetes mellitus: role of inflammation. Indian J Med Sci 2007;61:292-306.

54. Steffensen KR, Gustafsson JA. Putative metabolic effects of the liver X receptor (LXR). Diabetes 2004;53 Suppl 1:S36-S42.

55. Liao H, Langmann T, Schmitz G, Zhu Y. Native LDL upregulation of ATP-binding cassette transporter-1 in human vascular endothelial cells. Arterioscler Thromb Vasc Biol 2002;22:127-32.

56. Zhu Y, Liao H, Xie X et al. Oxidized LDL downregulates ATP-binding cassette transporter-1 in human vascular endothelial cells via inhibiting liver X receptor (LXR). Cardiovasc Res 2005;68:425-32.

57. Commerford SR, Vargas L, Dorfman SE et al. Dissection of the insulin-sensitizing effect of liver X receptor ligands. Mol Endocrinol 2007;21:3002-12.

58. Geyeregger R, Zeyda M, Stulnig TM. Liver X receptors in cardiovascular and metabolic disease. Cell Mol Life Sci 2006;63:524-39.

59. Zelcer N, Tontonoz P. Liver X receptors as integrators of metabolic and inflammatory signaling. J Clin Invest 2006;116:607-14.

60. Mitro N, Mak PA, Vargas L et al. The nuclear receptor LXR is a glucose sensor. Nature 2007;445:219-23.

61. Norton JD, Deed RW, Craggs G, Sablitzky F. Id helix-loop-helix proteins in cell growth and differentiation. Trends Cell Biol 1998;8:58-65.

62. Tamura Y, Sugimoto M, Ohnishi K, Sakai T, Hara E. Differential activity of a variant form of the human Id-1 protein generated by alternative splicing. FEBS Lett 1998;436:169-73.

63. Christy BA. A role for an alternatively spliced Id3 isoform in vascular lesions? Arterioscler Thromb Vasc Biol 2001;21:727-8.

64. Forrest S, McNamara C. Id family of transcription factors and vascular lesion formation. Arterioscler Thromb Vasc Biol 2004;24:2014-20.

65. Lim RW, Wu JM. Molecular mechanisms regulating expression and function of transcription regulator inhibitor of differentiation 3. Acta Pharmacol Sin 2005;26:1409-20.

66. Riechmann V, van C, I, Sablitzky F. The expression pattern of Id4, a novel dominant negative helix-loop-helix protein, is distinct from Id1, Id2 and Id3. Nucleic Acids Res 1994;22:749-55.

67. Benezra R, Rafii S, Lyden D. The Id proteins and angiogenesis. Oncogene 2001;20:8334-41.

68. Massari ME, Murre C. Helix-loop-helix proteins: regulators of transcription in eucaryotic organisms. Mol Cell Biol 2000;20:429-40.

69. Perk J, Iavarone A, Benezra R. Id family of helix-loop-helix proteins in cancer. Nat Rev Cancer 2005;5:603-14.

70. Wice BM, Bernal-Mizrachi E, Permutt MA. Glucose and other insulin secretagogues induce, rather than inhibit, expression of Id-1 and Id-3 in pancreatic islet beta cells. Diabetologia 2001;44:453-63.

71. Moreno PR, Fuster V. New aspects in the pathogenesis of diabetic atherothrombosis. J Am Coll Cardiol 2004;44:2293-300.

72. Luo B, Soesanto Y, McClain DA. Protein Modification by O-Linked GlcNAc Reduces Angiogenesis by Inhibiting Akt Activity in Endothelial Cells. Arterioscler Thromb Vasc Biol 2008.

73. Nishiyama K, Takaji K, Uchijima Y et al. Protein kinase A-regulated nucleocytoplasmic shuttling of Id1 during angiogenesis. J Biol Chem 2007;282:17200-9.

74. Sakurai D, Tsuchiya N, Yamaguchi A et al. Crucial role of inhibitor of DNA binding/differentiation in the vascular endothelial growth factor-induced activation and angiogenic processes of human endothelial cells. J Immunol 2004;173:5801-9.

75. Gronning LM, Tingsabadh R, Hardy K et al. Glucose induces increases in levels of the transcriptional repressor Id2 via the hexosamine pathway. Am J Physiol Endocrinol Metab 2006;290:E599-E606.

76. Berven L. Effects of hyperglycaemia in primary human macrophages. 2007. Department of Nutrition, Institute of Basic Medical services of the Faculty of Medicine, University of Oslo.
Ref Type: Thesis/Dissertation

77. Iyer SP, Akimoto Y, Hart GW. Identification and cloning of a novel family of coiled-coil domain proteins that interact with O-GlcNAc transferase. J Biol Chem 2003;278:5399-409.

78. Jaffe EA, Nachman RL, Becker CG, Minick CR. Culture of human endothelial cells derived from umbilical veins. Identification by morphologic and immunologic criteria. J Clin Invest 1973;52:2745-56.

79. Johansen LM. Effects of Methylglyoxal, TNFá and IL-1á on Proteoglycan Synthesis in Human Endothelial Cells *in vitro*. 2007. Faculty of Nutrition, Department of Nutrition, University of Oslo.
Ref Type: Thesis/Dissertation

80. Cheung AL. Isolation and Culture of Human Umbilical Vein Endothelial Cells (HUVEC). Current Protocols in Microbiology. A.4B.1. 2007. John Wely & Sons, Inc.
Ref Type: Report

81. Golks A, Tran TT, Goetschy JF, Guerini D. Requirement for O-linked N-acetylglucosaminyltransferase in lymphocytes activation. EMBO J 2007;26:4368-79.

82. Vanderford NL, Andrali SS, Ozcan S. Glucose induces MafA expression in pancreatic beta cell lines via the hexosamine biosynthetic pathway. J Biol Chem 2007;282:1577-84.

83. Kuo M, Zilberfarb V, Gangneux N, Christeff N, Issad T. O-GlcNAc modification of FoxO1 increases its transcriptional activity: a role in the glucotoxicity phenomenon? Biochimie 2008;90:679-85.

84. Yang WH, Kim JE, Nam HW et al. Modification of p53 with O-linked N-acetylglucosamine regulates p53 activity and stability. Nat Cell Biol 2006;8:1074-83.

85. Yao D, Taguchi T, Matsumura T et al. High glucose increases angiopoietin-2 transcription in microvascular endothelial cells through methylglyoxal modification of mSin3A. J Biol Chem 2007;282:31038-45.

86. Federici M, Lauro R. Review article: diabetes and atherosclerosis--running on a common road. Aliment Pharmacol Ther 2005;22 Suppl 2:11-5.

87. Du XL, Edelstein D, Rossetti L et al. Hyperglycemia-induced mitochondrial superoxide overproduction activates the hexosamine pathway and induces plasminogen activator inhibitor-1 expression by increasing Sp1 glycosylation. Proc Natl Acad Sci U S A 2000;97:12222-6.

88. Du XL, Edelstein D, Dimmeler S, Ju Q, Sui C, Brownlee M. Hyperglycemia inhibits endothelial nitric oxide synthase activity by posttranslational modification at the Akt site. J Clin Invest 2001;108:1341-8.

89. Varma S, Lal BK, Zheng R et al. Hyperglycemia alters PI3k and Akt signaling and leads to endothelial cell proliferative dysfunction. Am J Physiol Heart Circ Physiol 2005;289:H1744-H1751.

90. Bachetti T, Comini L, Curello S et al. Co-expression and modulation of neuronal and endothelial nitric oxide synthase in human endothelial cells. J Mol Cell Cardiol 2004;37:939-45.

91. Zeng G, Nystrom FH, Ravichandran LV et al. Roles for insulin receptor, PI3-kinase, and Akt in insulin-signaling pathways related to production of nitric oxide in human vascular endothelial cells. Circulation 2000;101:1539-45.

92. Gosmanov AR, Stentz FB, Kitabchi AE. De novo emergence of insulin-stimulated glucose uptake in human aortic endothelial cells incubated with high glucose. Am J Physiol Endocrinol Metab 2006;290:E516-E522.

93. Artwohl M, Brunmair B, Furnsinn C et al. Insulin does not regulate glucose transport and metabolism in human endothelium. Eur J Clin Invest 2007;37:643-50.

94. Deleu S, Savonet V, Behrends J, Dumont JE, Maenhaut C. Study of gene expression in thyrotropin-stimulated thyroid cells by cDNA expression array: ID3 transcription modulating factor as an early response protein and tumor marker in thyroid carcinomas. Exp Cell Res 2002;279:62-70.

95. Park SY, Ryu J, Lee W. O-GlcNAc modification on IRS-1 and Akt2 by PUGNAc inhibits their phosphorylation and induces insulin resistance in rat primary adipocytes. Exp Mol Med 2005;37:220-9.

96. Gandy JC, Rountree AE, Bijur GN. Akt1 is dynamically modified with O-GlcNAc following treatments with PUGNAc and insulin-like growth factor-1. FEBS Lett 2006;580:3051-8.

97. Kim HS, Kim EM, Lee J et al. Heat shock protein 60 modified with O-linked N-acetylglucosamine is involved in pancreatic beta-cell death under hyperglycemic conditions. FEBS Lett 2006;580:2311-6.

98. Taylor RP, Parker GJ, Hazel MW et al. Glucose Deprivation Stimulates O-GlcNAc Modification of Proteins through Up-regulation of O-Linked N-Acetylglucosaminyltransferase. J Biol Chem 2008;283:6050-7.

99. Cheung WD FAU - Hart G, Hart GW. AMP-activated protein kinase and p38 MAPK activate O-GlcNAcylation of neuronal proteins during glucose deprivation.

100. Baudin B, Bruneel A, Bosselut N, Vaubourdolle M. A protocol for isolation and culture of human umbilical vein endothelial cells. Nat Protoc 2007;2:481-5.

101. Wells L, Vosseller K, Hart GW. A role for N-acetylglucosamine as a nutrient sensor and mediator of insulin resistance. Cell Mol Life Sci 2003;60:222-8.

102. Fulop N, Feng W, Xing D et al. Aging leads to increased levels of protein O-linked N-acetylglucosamine in heart, aorta, brain and skeletal muscle in Brown-Norway rats. Biogerontology 2008;9:139-51.

103. Pearce KL, Noakes M, Keogh J, Clifton PM. Effect of carbohydrate distribution on postprandial glucose peaks with the use of continuous glucose monitoring in type 2 diabetes. Am J Clin Nutr 2008;87:638-44.

104. Rendell MS, Jovanovic L. Targeting postprandial hyperglycemia. Metabolism 2006;55:1263-81.

105. Quagliaro L, Piconi L, Assaloni R et al. Intermittent high glucose enhances ICAM-1, VCAM-1 and E-selectin expression in human umbilical vein endothelial cells in culture: the distinct role of protein kinase C and mitochondrial superoxide production. Atherosclerosis 2005;183:259-67.

106. Yamamoto T, Shimano H, Inoue N et al. Protein kinase A suppresses sterol regulatory element-binding protein-1C expression via phosphorylation of liver X receptor in the liver. J Biol Chem 2007;282:11687-95.

107. Li X, Zhang S, Blander G, Tse JG, Krieger M, Guarente L. SIRT1 deacetylates and positively regulates the nuclear receptor LXR. Mol Cell 2007;28:91-106.

108. Ghisletti S, Huang W, Ogawa S et al. Parallel SUMOylation-dependent pathways mediate gene- and signal-specific transrepression by LXRs and PPARgamma. Mol Cell 2007;25:57-70.

109. Pammer J, Reinisch C, Kaun C, Tschachler E, Wojta J. Inhibitors of differentiation/DNA binding proteins Id1 and Id3 are regulated by statins in endothelial cells. Endothelium 2004;11:175-80.

110. Neal MJ. Madical Pharmacology at a Glance. Wiley Blackwell, 2002.

111. Matsumura ME, Li F, Berthoux L et al. Vascular injury induces posttranscriptional regulation of the Id3 gene: cloning of a novel Id3 isoform expressed during vascular lesion formation in rat and human atherosclerosis. Arterioscler Thromb Vasc Biol 2001;21:752-8.

112. Gahr SA, Weber GM, Rexroad CE, III. Fasting and refeeding affect the expression of the Inhibitor of DNA Binding (ID) genes in rainbow trout (Oncorhynchus mykiss) muscle. Comp Biochem Physiol B Biochem Mol Biol 2006;144:472-7.

113. Andrali SS, Qian Q, Ozcan S. Glucose mediates the translocation of NeuroD1 by O-linked glycosylation. J Biol Chem 2007;282:15589-96.

114. Takeda T, Sakata M, Isobe A et al. Involvement of Sp-1 in the regulation of the Id-1 gene during trophoblast cell differentiation. Placenta 2007;28:192-8.

115. Pagliuca A, Cannada-Bartoli P, Lania L. A role for Sp and helix-loop-helix transcription factors in the regulation of the human Id4 gene promoter activity. J Biol Chem 1998;273:7668-74.

116. Jain RK, Finn AV, Kolodgie FD, Gold HK, Virmani R. Antiangiogenic therapy for normalization of atherosclerotic plaque vasculature: a potential strategy for plaque stabilization. Nat Clin Pract Cardiovasc Med 2007;4:491-502.

117. Virmani R, Kolodgie FD, Burke AP et al. Atherosclerotic plaque progression and vulnerability to rupture: angiogenesis as a source of intraplaque hemorrhage. Arterioscler Thromb Vasc Biol 2005;25:2054-61.

118. Chi JT, Chang HY, Haraldsen G et al. Endothelial cell diversity revealed by global expression profiling. Proc Natl Acad Sci U S A 2003;100:10623-8.

119. Puente Navazo MD FAU - Chettab, Chettab KF, Duhault JF, Koenig-Berard E FAU - McGregor, McGregor JL. Glucose and insulin modulate the capacity of endothelial cells (HUVEC) to express P-selectin and bind a monocytic cell line (U937).

7. Tables

Table 1. Complete MCDB culture medium

Ingredients	Final concentration
EBM-media M-8537 (MCDB-131 medium)	Powder for 1000 ml
Epidermal growth factor (EGF)	10 ng/ml
Fibroblast growth factor (FGF)	1 ng/ml
Hydrocortisone	1 µg/ml
Fungisone	250 ng/ml
Gentamycin	50 µg/ml
Foetal bovine serum (FBS) (heat inactivated)	7 %

The D-glucose concentration in baseline EBM is 5 mM.

Table 2. Transporting buffer

Ingredients	Final concentration
1x PBS (sterile)	1000 ml
Streptomycin sulphate	50 mg/l

Stored at 4^{o}C

Table 3. 10x PBS, pH 6.8

Ingredients	Final concentration
NaH_2PO_4 x $2H_2O$	4,832 mM
KH_2PO_4	1,937 mM
NaCl	1,454 M

Table 4. RIPA-buffer

Ingredients	Final concentration
NP-40	1 %
SDS	0.1 %
NaCl	0.15 M
Tris-HCl	50 mM
Na-deoxycholate	0.5 %
AEBSF	1 mM
NAG-thiazoline	1 µM
Protease inhibitors	1 tablet pr. 10 ml
ALLN	1/100 – 1/400 µl

Table 5. Loading buffer (1x)

Ingredients	Final concentration
Tris pH 6.8	40 mM
SDS	0.8 %
Glycerol	4 %
Bromphenol Blue	0.025 %

Table 6. Lysis buffer

Ingredients	Final concentration
NP-40	0.2 %
1x PBS	96,68 %
DTT	1 mM

AEBSF	1 mM
NAG-thiazoline	1 µM
Protease inhibitors	1 tablet pr. 10 ml
ALLN	1/100 – 1/400 µl
NaF	50 mM
NaPPi	0.01 M
N_3VO_4	0.001 M

Table 7. NE2 lysis buffer

Ingredients	**Final concentration**
Hepes pH 7.9	20 mM
$MgCl_2$	1.5 mM
NaCl	420 mM
Glycerol	25 %
EDTA	0.2 mM
DTT	1 mM
AEBSF	1 Mm
NAG-thiazoline	1 µM
Protease inhibitors	1 tablet pr. 10 ml
ALLN	1/100 – 1/400
NaF	50 mM
NaPPi	0.01 M
N_3VO_4	0.001 M

Table 8. BSA standard samples

Well	BSA (2 mg/ml)	MQ-H_2O	Lysis buffer	A+B solution
A	0 µl	45 µl	5 µl	200 µl
B	0 µl	45 µl	5 µl	200 µl
C	3 µl	42 µl	5 µl	200 µl
D	3 µl	42 µl	5 µl	200 µl
E	5 µl	40 µl	5 µl	200 µl
F	5 µl	40 µl	5 µl	200 µl
G	8 µl	37 µl	5 µl	200 µl
H	8 µl	37 µl	5 µl	200 µl

Table 9. Running buffer (10x) for western blotting

Ingredients	Final concentration
Trizma base	0.25 M
Glycine	1.92 M
SDS	1%

Table 10A. Transfer (Blotting) buffer (10x) for western blotting

Ingredients	Final concentration
Trizma base	0.25 M
Glycine	1.92 M

pH should be 8.3; do not adjust

Table 10B. Transfer (Blotting) buffer (1x)

Ingredients	Final concentration
Methanol	10 % - 20 %
10x transfer buffer	1x

Table 11. Stripping buffer

Ingredients	Final concentration
B-Mercaptoethanol	100 mM
Tris-HCL, pH 6.8	62.5 mM
SDS	2 %

Table 12A. TBS (10x)

Ingredients	Final concentration
Trizma HCl	0.2 M
NaCl	1,37 M

Adjust pH to 7.6 with pure HCl

Table 12B. TBST (1x)

Ingredients	Final concentration
10x TBS	1x
Tween 20	0.1 %

8. Appendix

8.1 Appendix A

YinOYang 1.2 Prediction Results

```
The predictions for Yin-Yang sites in 1 sequence
(NetPhos threshold used: 0.5)


Name:  LXRa    Length:  447
MSLWLGAPVPDIPPDSAVELWKPGAQDASSQAQGGSSCILREEARMPHSAGGTAGVGLEAAEPTALLTRAEPPSE
PTEIR      80
PQKRKKGPAPKMLGNELCSVCGDKASGFHYNVLSCEGCKGFFRRSVIKGAHYICHSGGHCPMDTYMRRKCQECRL
RKCRQ     160
AGMREECVLSEEQIRLKKLKRQEEEQAHATSLPPRASSPPQILPQLSPEQLGMIEKLVAAQQQCNRRSFSDRLRV
TPWPM     240
APDPHSREARQQRFAHFTELAIVSVQEIVDFAKQLPGFLQLSREDQIALLKTSAIEVMLLETSRRYNPGSESITF
LKDFS     320
YNREDFAKAGLQVEFINPIFEFSRAMNELQLNDAEFALLIAISIFSADRPNVQDQLQVERLQHTYVEALHAYVSI
HHPHD     400
RLMFPRMLMKLVSLRTLSSVHSEQVFALRLQDKKLPPLLSEIWDVHE
.............................GY.............................................Y.
.....      80
.....     160
.............................G.....GY.....................................
Y....     240
.....Y.....................................................................
.....     320
.....     400
.........................................


-------------------------------------------------------------------------
----
SeqName     Residue  O-GlcNAc  Potential  Thresh.  Thresh.   NetPhos
YinOYang?
                     result    (o-glcnac)   (1)      (2)    potential
                                                           (Thresh=0.5)
-------------------------------------------------------------------------
----
LXRa           29  S    ++       0.5211    0.3889   0.4746
LXRa           30  S*   +++      0.7051    0.3900   0.4761     0.724
*
LXRa           74  S*   +++      0.5767    0.3561   0.4304     0.573
*
LXRa          191  S    ++       0.5821    0.4139   0.5083
LXRa          197  S    +++      0.6534    0.3779   0.4598
LXRa          198  S*   +        0.4449    0.3766   0.4581     0.981
*
LXRa          236  T*   ++       0.5666    0.4454   0.5508     0.741
*
LXRa          246  S*   ++       0.5422    0.3834   0.4672     0.955
*
-------------------------------------------------------------------------
----
```

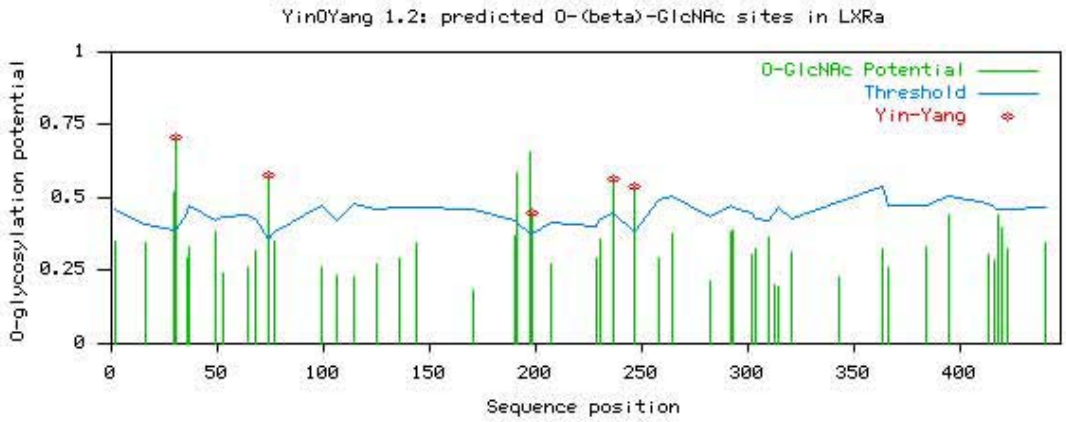
YinOYang 1.2: predicted O-(beta)-GlcNAc sites in LXRa
O-GlcNAc Potential
Threshold
Yin-Yang
O-glycosylation potential
1
0.75
0.5
0.25
0
0
50
100
150
200
250
300
350
400
Sequence position

8.2 Appendix B

YinOYang 1.2 Prediction Results

```
The predictions for Yin-Yang sites in 1 sequence
(NetPhos threshold used: 0.5)


Name:  LXRb    Length:  461
MSSPTTSSLDTPLPGNGPPQPGAPSSSPTVKEEGPEPWPGGPDPDVPGTDEASSACSTDWVIPDPEEEPERKRKK
GPAPK      80
MLGHELCRVCGDKASGFHYNVLSCEGCKGFFRRSVVRGGARRYACRGGGTCQMDAFMRRKCQQCRLRKCKEAGMR
EQCVL     160
SEEQIRKKKIRKQQQQESQSQSQSPVGPQGSSSSASGPGASPGGSEAGSQGSGEGEGVQLTAAQELMIQQLVAAQ
LQCNK     240
RSFSDQPKVTPWPLGADPQSRDARQQRFAHFTELAIISVQEIVDFAKQVPGFLQLGREDQIALLKASTIEIMLLE
TARRY     320
NHETECITFLKDFTYSKDDFHRAGLQVEFINPIFEFSRAMRRLGLDDAEYALLIAINIFSADRPNVQEPGRVEAL
QQPYV     400
EALLSYTRIKRPQDQLRFPRMLMKLVSLRTLSSVHSEQVFALRLQDKKLPPLLSEIWDVHE
.GG..YY.................YG.....................G...G.....................
.....      80
........................................................................
.....     160
.................Y.Y.G........GGY...........G.............................
.....     240
.........Y.........G.....................................................
.....     320
........................................................................
.....     400
............................................................


-------------------------------------------------------------------------
----
SeqName     Residue  O-GlcNAc  Potential  Thresh.  Thresh.   NetPhos
YinOYang?
                     result   (o-glcnac)   (1)      (2)    potential
                                                          (Thresh=0.5)
-------------------------------------------------------------------------
----
LXRb           2   S    +++      0.5768    0.3654   0.4430
LXRb           3   S    ++       0.5136    0.3743   0.4550
LXRb           6   T*   +++      0.5987    0.4042   0.4952     0.554
*
LXRb           7   S*   ++       0.5002    0.4045   0.4956     0.994
*
LXRb          25   S*   ++       0.5147    0.3808   0.4637     0.646
*
LXRb          26   S    ++       0.5651    0.3837   0.4676
LXRb          49   T    ++       0.5322    0.3906   0.4769
LXRb          53   S    +        0.4998    0.4101   0.5032
LXRb         178   S*   +++      0.7347    0.3573   0.4320     0.507
*
LXRb         180   S*   ++       0.5389    0.3658   0.4435     0.917
*
LXRb         182   S    +        0.3778    0.3717   0.4514
LXRb         191   S    +++      0.5798    0.3918   0.4785
```

LXRb	192	S	+++	0.7070	0.3969	0.4854	
LXRb	193	S*	++	0.5374	0.4013	0.4914	0.840
*							
LXRb	205	S	++	0.5777	0.3975	0.4862	
LXRb	250	T*	++	0.5122	0.4065	0.4984	0.565
*							
LXRb	260	S	+++	0.5882	0.3736	0.4539	

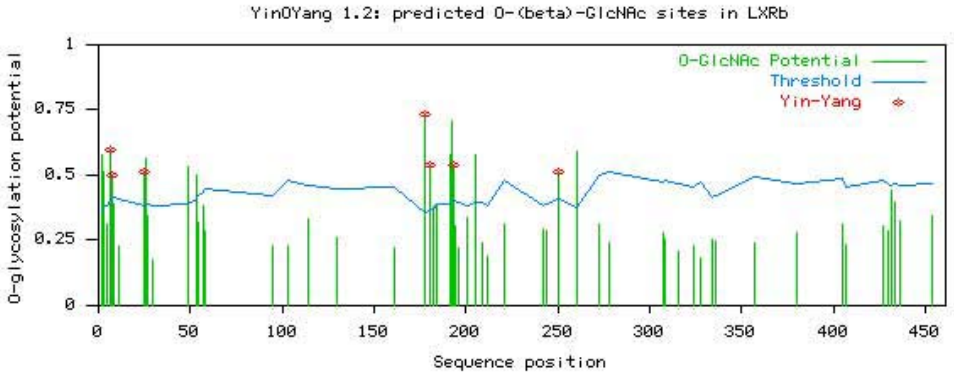

8.3 Appendix C

YinOYang 1.2 Prediction Results

```
The predictions for Yin-Yang sites in 1 sequence
(NetPhos threshold used: 0.5)


Name:  Id1     Length:  155
MKVASGSTATAAAGPSCALKAGKTASGAGEVVRCLSEQSVAISRCAGGAGARLPALLDEQQVNVLLYDMNGCYSR
LKELV      80
PTLPQNRKVSKVEILQHVIDYIRDLQLELNSESEVGTPGGRGLPVRAPLSTLNGEISALTAEAACVPADDRILCR
.......G.G.....G.............................................................
.....      80
.............................G..................Y.......................


-------------------------------------------------------------------------------
----
SeqName     Residue  O-GlcNAc  Potential  Thresh.  Thresh.   NetPhos
YinOYang?
                     result   (o-glcnac)   (1)      (2)     potential
                                                          (Thresh=0.5)
-------------------------------------------------------------------------------
----
Id1             8  T    +        0.4433    0.3761   0.4574
Id1            10  T    +        0.3827    0.3820   0.4653
Id1            16  S    +++      0.6192    0.4017   0.4918
Id1           111  S    +        0.3529    0.3507   0.4231
Id1           130  S*   +        0.4660    0.4067   0.4986      0.625
*
-------------------------------------------------------------------------------
----
```

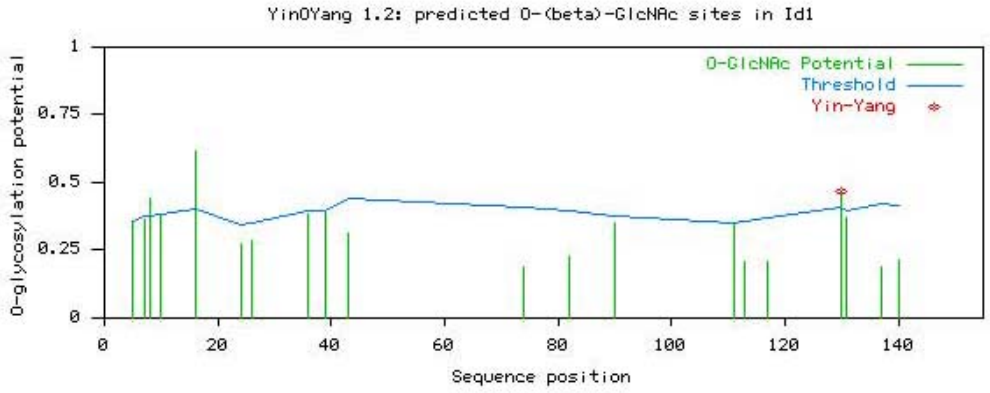

8.4 Appendix D

YinOYang 1.2 Prediction Results

```
The predictions for Yin-Yang sites in 1 sequence
(NetPhos threshold used: 0.5)

Name:  Id3     Length:  119
MKALSPVRGCYEAVCCLSERSLAIARGRGKGPAAEEPLSLLDDMNHCYSRLRELVPGVPRGTQLSQVEILQRVID
YILDL      80
QVVLAEPAPGPPDGPHLPIQTAELAPELVISNDKRSFCH
................................................................................
.....      80
.....................................G...

-------------------------------------------------------------------------------
----
SeqName     Residue  O-GlcNAc  Potential  Thresh.  Thresh.   NetPhos
YinOYang?
                     result   (o-glcnac)   (1)      (2)    potential
                                                          (Thresh=0.5)
-------------------------------------------------------------------------------
----
Id3           116  S    +        0.3348    0.3303   0.3956
-------------------------------------------------------------------------------
----
```